

Discovery of Piragliatin—First Glucokinase Activator Studied in Type 2 Diabetic Patients

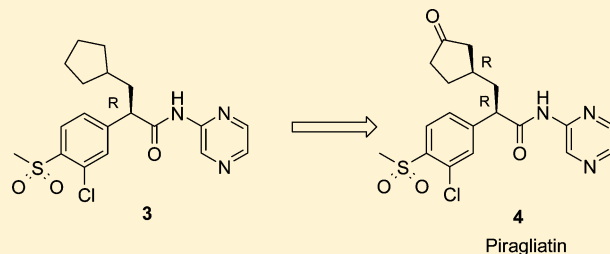
Ramakanth Sarabu,^{*,†} Fred T. Bizzarro,[†] Wendy L. Corbett,[†] Mark T. Dvorozniak,[†] Wanping Geng,[†] Joseph F. Grippo,[†] Nancy-Ellen Haynes,[†] Stanley Hutchings,[†] Lisa Garofalo,[†] Kevin R. Guertin,[†] Darryl W. Hilliard,[†] Marek Kabat,[†] Robert F. Kester,[†] Wang Ka,[†] Zhenmin Liang,[†] Paige E. Mahaney,[†] Linda Marcus,[†] Franz M. Matschinsky,[‡] David Moore,[†] Jagdish Racha,[†] Roumen Radinov,[†] Yi Ren,[†] Lida Qi,[†] Michael Pignatello,[†] Cheryl L. Spence,[†] Thomas Steele,[†] John Teng,[†] and Joseph Grimsby[†]

[†]Hoffmann-La Roche Inc., pRED, Pharma Research & Early Development, DTA Metabolism, 340 Kingsland Street, Nutley, New Jersey 07110, United States

[‡]Department of Biochemistry and Diabetes Center, University of Pennsylvania School of Medicine, Philadelphia, Pennsylvania 19104, United States

S Supporting Information

ABSTRACT: Glucokinase (GK) activation as a potential strategy to treat type 2 diabetes (T2D) is well recognized. Compound 1, a glucokinase activator (GKA) lead that we have previously disclosed, caused reversible hepatic lipidosis in repeat-dose toxicology studies. We hypothesized that the hepatic lipidosis was due to the structure-based toxicity and later established that it was due to the formation of a thiourea metabolite, 2. Subsequent SAR studies of 1 led to the identification of a pyrazine-based lead analogue 3, lacking the thiazole moiety. In vivo metabolite identification studies, followed by the independent synthesis and profiling of the cyclopentyl keto- and hydroxyl- metabolites of 3, led to the selection of piragliatin, 4, as the clinical lead. Piragliatin was found to lower pre- and postprandial glucose levels, improve the insulin secretory profile, increase β -cell sensitivity to glucose, and decrease hepatic glucose output in patients with T2D.



INTRODUCTION

Glucokinase (GK) activation as a potential strategy to treat type 2 diabetes (T2D) is now well recognized.¹ GK, also called hexokinase IV, is a glycolytic enzyme that catalyzes the oxidative phosphorylation of glucose by adenosine triphosphate (ATP). GK responds functionally to plasma glucose fluctuations observed during pre- and postprandial periods. This enables pancreatic β -cell GK to function as a molecular sensor² that couples changes in blood glucose levels with insulin release to maintain glucose homeostasis. As a sensor, GK determines the rate and threshold concentration of glucose (~ 5 mM in healthy individuals) required to initiate the signaling cascade leading to insulin release. In the liver, GK catalyzes the first step in glucose metabolism and plays an important role in determining net glucose utilization and production in this organ.³ GK is also expressed in pancreatic α -cells, entero-endocrine K and L cells, glucose-excited/glucose-inhibited neurons of the hypothalamus and brainstem, and anterior pituitary cells, but its physiological role in these tissues is less well understood.⁴

Loss-of-function mutations in one or both alleles of the GK gene cause maturity onset diabetes of the young type 2 (MODY-2) and permanent neonatal diabetes mellitus, respectively.⁵ In contrast, a gain-of-function mutation in a

single GK allele causes persistent hyperinsulinemic hypoglycemia of infancy (PHHI) due to excessive insulin release.⁶ On the basis of the pivotal role of GK as a glucose sensor in pancreatic β -cells and its key role in regulating glucose production in liver, allosteric activators of this enzyme are being actively pursued as antidiabetic agents. We previously disclosed the discovery of RO0281675, 1, an archetypal glucokinase activator (GKA), its efficacy profile in mouse models of T2D, and its effect on improving glycemic control in healthy volunteers administered a single oral dose (25–400 mg) (Figure 1).⁷ However, compound 1 was unsuitable as a full development candidate due to its narrow safety margin in preclinical toxicology studies. In this report, we disclose efforts to eliminate this liability leading to the discovery of piragliatin,⁸ a potent and efficacious GKA that was advanced to phase 2 clinical trials in T2D patients.

Compound 1 caused reversible hepatic lipidosis in repeat-dose toxicology studies in rats and dogs. We hypothesized that the hepatic lipidosis was due to structure-based toxicity and investigated if the formation of a reactive metabolite from either the parent molecule or its metabolite could be the causative

Received: January 25, 2012

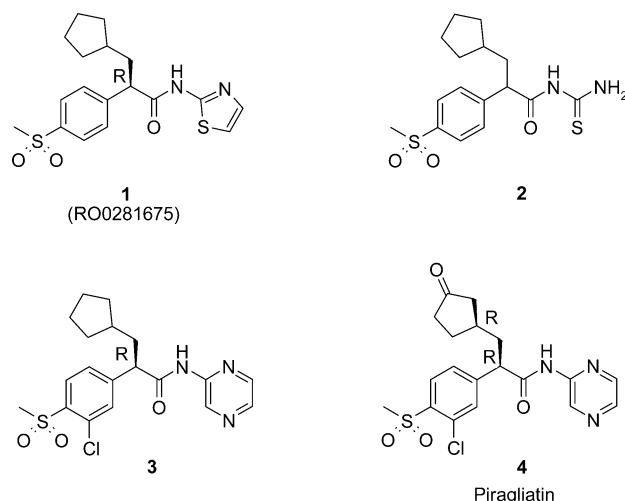


Figure 1. Structures of GK activators and the thiourea metabolite 2.

agent. These investigations provided strong evidence that the hepatic lipidosis was due to the formation of a thiourea metabolite, 2, of compound 1 and not due to the mechanism of action. Further efforts to identify a 4,5- disubstituted or 4- or 5- monosubstituted thiazole analogue of 1 unable to form a thiourea metabolite, while maintaining the potency and adequate pharmacokinetic properties, were unsuccessful. Subsequent SAR studies of 1 led to the identification of a pyrazine-based lead analogue 3 lacking the thiazole moiety. In vivo metabolic identification studies revealed a number of oxidative metabolites of compound 3 at the cyclopentyl ring. Independent synthesis of the cyclopentyl keto- and hydroxyl-metabolites and their in vitro and in vivo safety and efficacy profiling led to the selection of piragliatin, 4, as the clinical lead (Figure 1). Subchronic and chronic toxicology studies in rats and canines with Piragliatin revealed no evidence of hepatic lipidosis (unpublished results). Piragliatin was found to lower pre- and postprandial glucose levels, improve the insulin secretory profile, increase β -cell sensitivity to glucose, and decrease hepatic glucose output in patients with T2D.

CHEMISTRY

The general synthetic strategy used to prepare the various aryl acetamides is shown in Scheme 1, which consists of preparing the corresponding arylpropionic acid or ester and subsequent alkylation with cyclopentylmethyl iodide, followed by hydrolysis of the ester group and coupling with the corresponding aminoheterocycle.^{7b} The syntheses of thiourea analogue 2, the thiazole analogues of 1 shown in Table 3 (compounds 5–11), the aryl substitution analogues shown in Table 4 (compounds 12–18), and the analogues shown in Table 5 for SAR

comparison between chloro- and *des*-chloro (compounds 19–26) are described in the Supporting Information.

Compound 3 was prepared in a seven-step stereoselective synthesis outlined in Scheme 2. Hydrolysis of 37b afforded pyruvate 60, which was then deoxygenated under hydrazine hydrate/potassium hydroxide conditions, leading to the formation of the arylacetic acid 61. The subsequent transformations were (a) preparation of a chiral amide with (1*R*, 2*R*)-(-)-pseudoephedrine, (b) diastereoselective alkylation,⁹ and (c) hydrolysis of the amide to yield the carboxylic acid intermediate 64. The thiomethyl of compound 64 was oxidized to the key methylsulfone intermediate 65, which was then coupled with 2-aminopyrazine to yield compound 3.

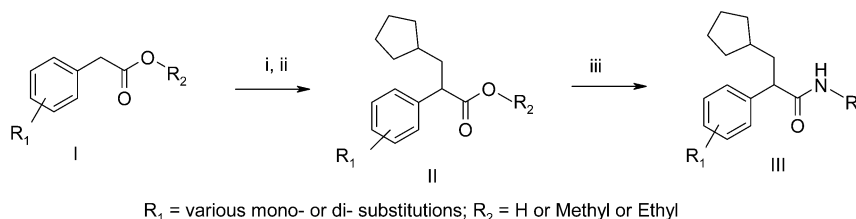
The synthesis of the oxidative metabolites of 3 required the synthesis of protected 2- and 3-hydroxyl-cyclopentyl methyl iodides, 69 and 72, respectively. The iodide 69 was accessible from 2-hydroxycyclopentyl carboxylic acid ethyl ester, 66, in three steps: (a) protection of hydroxyl group as tetrahydropyranyl ether, (b) reduction of the ethyl ester to hydroxyl methyl group, and (c) conversion of hydroxyl methyl to the cyclopentylmethyl iodide analogue 69. The 3-cyclopentylmethyl iodide, 72, was synthesized starting from the reported 3-iodomethyl cyclopentanone.¹⁰ The two steps consists of (a) reduction of the ketone followed by (b) the protection of the resulting alcohol as a tetrahydropyranyl ether (Scheme 3).

The diastereomeric mixtures of cyclopentyl 2-hydroxy 27 and 2-ketone 29 metabolites were prepared in a synthetic sequence outlined in Scheme 4. The sequence started with the diastereoselective alkylation of chiral acetamide 62 with the protected cyclopentylmethyl iodide derivative, 69, to yield a mixture of alkylated diastereomers, 73. These diastereomers were transformed to the key 2-keto-carboxylic acid intermediate, 76, in three steps consisting of (a) removal of the tetrahydropyranyl- group, (b) oxidation of the resulting cyclopentyl 2-hydroxy- derivatives 74 to ketones, 75, and then, (c) removal of pseudoephedrine chiral auxiliary via acid hydrolysis. The thiomethyl moiety in cyclopentyl 2-ketone diastereomers 76 was oxidized to the corresponding sulfone 78 in a two-step procedure, which was then coupled with 2-aminopyrazine to yield the 2-keto-metabolite diastereomeric mixture 29. The corresponding mixture of diastereomeric cyclopentyl 2-hydroxy metabolites 27 was readily accessible via a sodium borohydride reduction of 29.

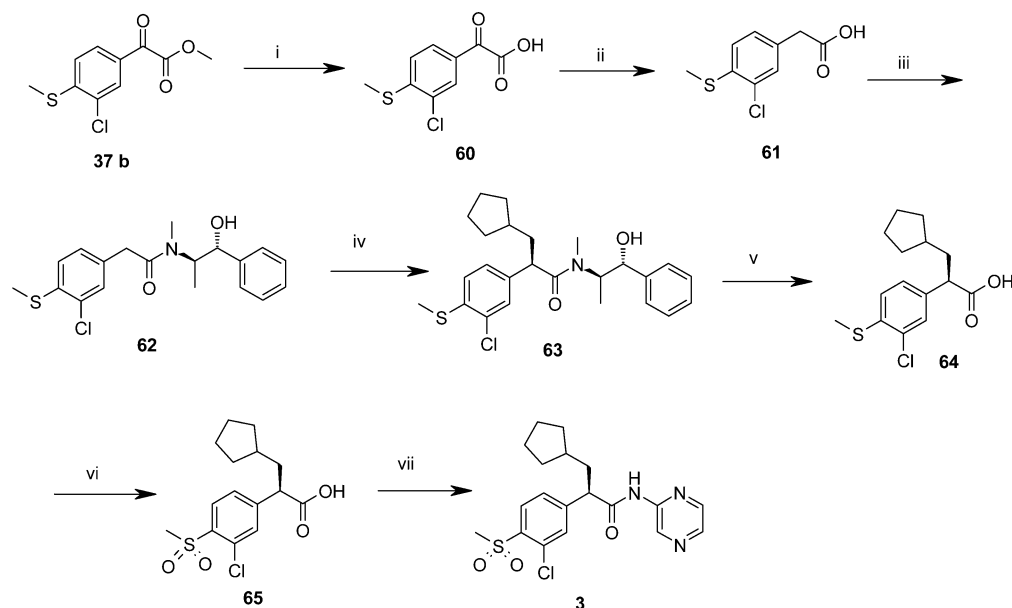
In an analogous manner, the 3-hydroxyl 28 and 3-ketone 30 diastereomeric mixtures were prepared starting from the chiral amide intermediate 62 and the 3-(2-tetrahydropyranyl)-oxy-cyclopentyl derivative 72, in a six-step sequence (Scheme 5).

Both the *R,S*-31 and the *R,R*-4 diastereomers corresponding to the C3-keto metabolites of 3 were available via stereoselective syntheses starting from either *S,S*-84 or *R,R*-91 hydrobenzoin ketals of cyclopent-2-enone. The key

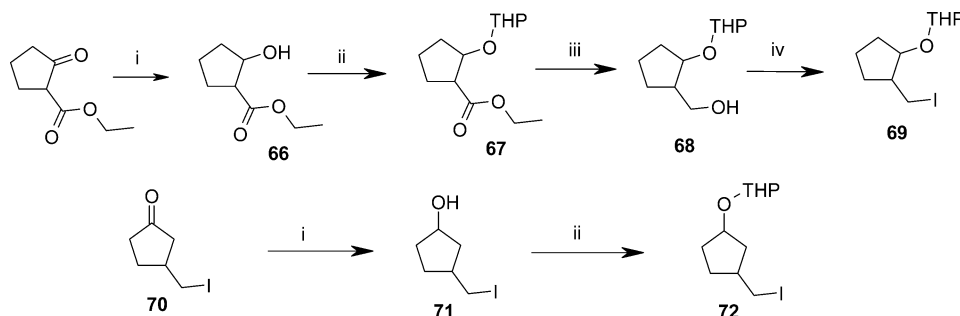
Scheme 1. General Synthetic Strategy^a



^aConditions: (i) alkylation, (ii) hydrolysis, and (iii) 2-amino-heterocycle coupling.

Scheme 2. Synthesis of Compound 3^a

^aReagents and conditions: (i) Aqueous NaOH, toluene, 60 °C, 2.5 h, 98%. (ii) N₂H₄, KOH, 16 h, 89%. (iii) K₂CO₃, (1R,2R)-(-)-pseudoephedrine, Cl₃COCl, acetone, -10 to 25 °C, ethyl acetate recrystallization, 78%. (iv) HMDS, *n*-BuLi, THF, cyclopentylmethyl iodide, -45 to 0 to 25 °C, DMPU, 67%. (v) 9 N H₂SO₄, 98%. (vi) HCOOH, 30% H₂O₂, 16 h, 80%. (vii) (COCl)₂, 1 drop DMF, CH₂Cl₂, 2-aminopyrazine, pyridine, 0–25 °C, THF, 16 h, 70%.

Scheme 3. Synthesis of Oxygentated Cyclopentyl Methyl Iodides^a

^aReagents and conditions for 69: (i) NaBH₄, EtOH, 84%. (ii) 3,4-Dihydro-(2H)-pyran, pyridinium PTS, CH₂Cl₂, 5 h, 88%. (iii) LiAlH₄, THF, 0–25 °C, 18 h, 84%. (iv) Ph₃P, imidazole, I₂, CH₂Cl₂, 0–25 °C, 3 h, 75%. Reagents and conditions for 72: (i) NaBH₄, CH₃OH, 0 °C, 0.75 h, 59%. (ii) 3,4-Dihydro-(2H)-pyran, pyridinium PTS, CH₂Cl₂, 25 °C, 24 h, 75%.

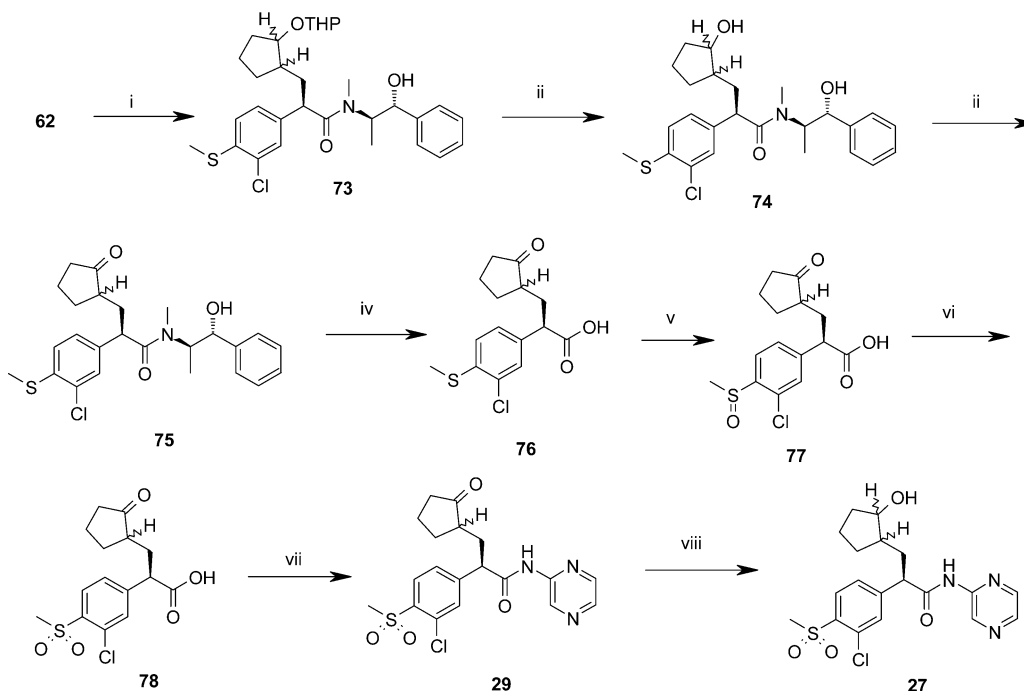
transformations in the synthesis of piragliatin 4 were (a) the high-yielding stereoselective Simmons–Smith cyclopropanation reaction¹¹ of the chiral ketal 91 to the corresponding bicyclic intermediate 92, (b) trimethylsilyl iodide-catalyzed opening of the cyclopropane¹² 92 to the alkyl iodide 93, and (c) the diastereoselective alkylation of chiral amide 62 with alkyl iodide 93 to yield the chiral alkylated phenyl acetamides 94. The remaining sequence of reactions was similar to that described for compound 29 (Scheme 6).

RESULTS AND DISCUSSION

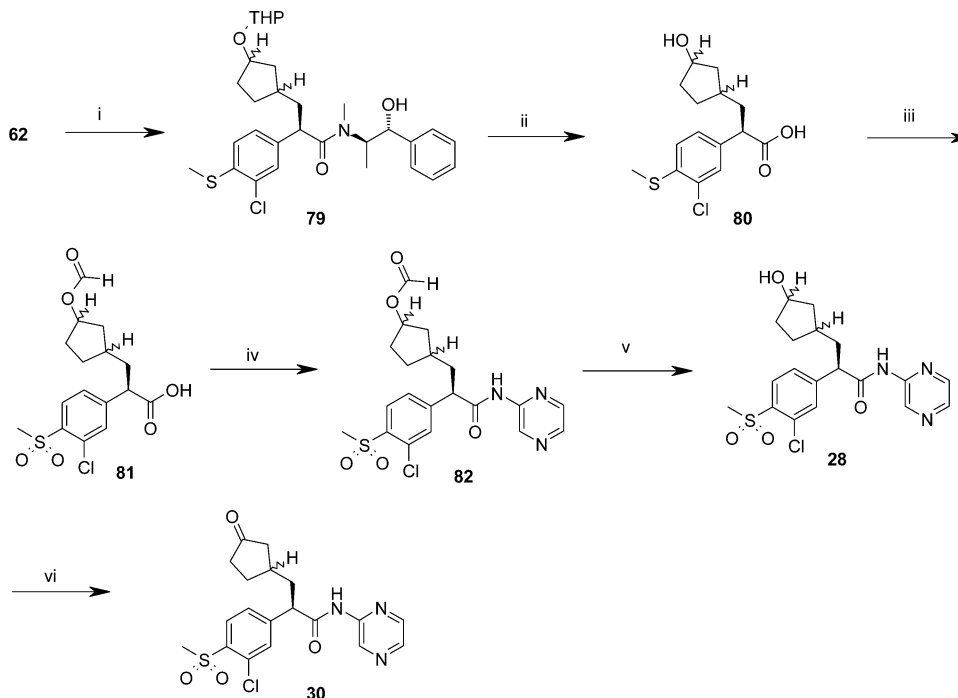
The archetypal GKA 1 was found to cause reversible hepatic lipidosis in rats and dogs and was unsuitable for chronic therapeutic use. To determine whether lipidosis was due to GK activation¹³ or the compound structure-based toxicity, we explored if a putative reactive metabolite arising from either the parent molecule or its metabolite could be the causative agent. The metabolite profile of 1 in mouse, rat, dog, monkey, and human liver microsomal incubation studies identified the

formation of oxidative metabolites corresponding to the cyclopentyl group [i.e., hydroxy (M2, M3) and ketone (M4) products] and the thiourea metabolites (M1, M5, and M6) corresponding to the parent, and the cyclopentyl hydroxy metabolite (Table 1 and Figure 2) and an unidentified metabolite M7.

The thiourea metabolites (M1, M5, and M6) were suspected to be the causative agents of hepatic lipidosis, based on literature reports on liver toxicity.¹⁴ We used the ent-1 (the *S* enantiomer of 1), which does not activate GK or lower glucose levels,² and the racemic thiourea 2 (M6) (SC_{1.5} = 45 μM) as structural probes to investigate the lipidosis. We conducted 5 day and acute (single dose) toxicity studies with compounds 1, ent-1, and 2 (Table 2). In the 5 day studies, glucose levels on day 3 and hepatic lipidosis at the end of the study were evaluated. All three compounds (1, ent-1, and 2) were found to cause hepatic lipidosis as observed through Oil Red O staining, and glucose lowering was observed only with compound 1 (Figures 1 and 2 in the Supporting Information). A single dose

Scheme 4. Synthesis of 2-Hydroxy (27) and 2-Keto (29) Metabolites of Compound 3^a

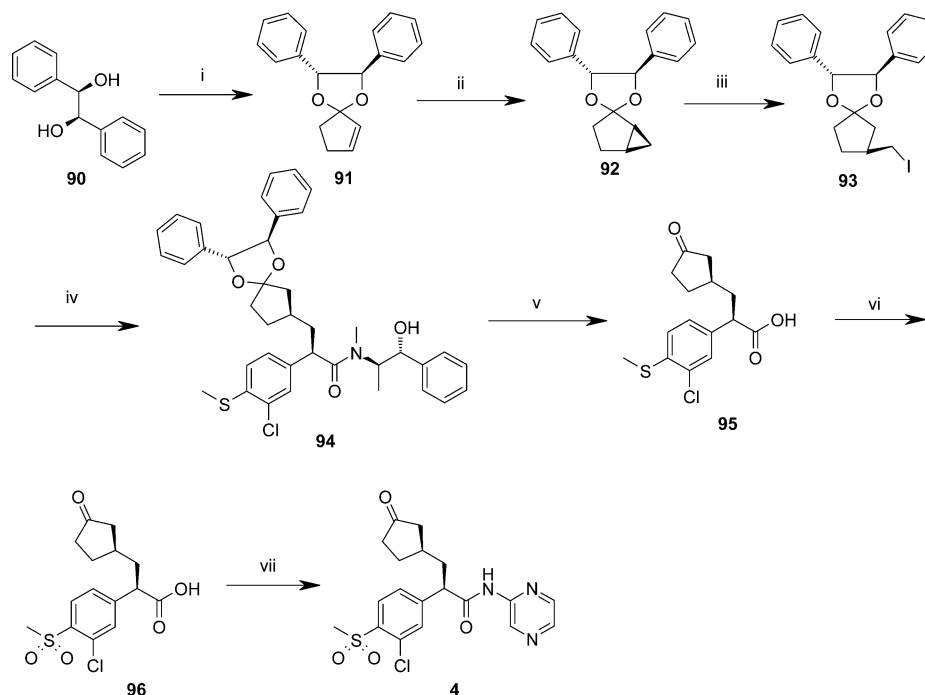
^aReagents and conditions: (i) HMDS, *n*-BuLi, THF, **69**, −45 to 0 to 25 °C, DMPU, 71%. (ii) Pyridinium-PTS, 50 °C, 2 h, EtOH, 93%. (iii) *N*-Methyl-morpholine-*N*-oxide, tetrapropylammonium perruthenate, molecular sieves, CH₂Cl₂, 25 °C, 20 min, 77%. (iv) 18 M HCl, 120 °C, 18 h, 82%. (v) HCOOH, 30% H₂O₂, water, 0 °C, 1 h, 100%. (vi) KMnO₄, water, CH₃OH, 25 °C, 1 h, 43%. (vii) (COCl)₂, 1 drop DMF, CH₂Cl₂, 2-aminopyrazine, pyridine, 0–25 °C, THF, 1 h, 51%. (viii) NaBH₄, 0 °C, 20 min, EtOH, 76%.

Scheme 5. Synthesis of 3-Hydroxy (29) and 3-Keto (31) Metabolites of 3^a

^aReagents and conditions: (i) HMDS, *n*-BuLi, **72**, −45 to 0 to 25 °C, 4 h, DMPU, THF, 91%. (ii) 9 N H₂SO₄, dioxane, reflux, 15 h, 44%. (iii) HCOOH, 30% H₂O₂, 16 h, 103%. (iv) (COCl)₂, DMF (2 drops), CH₂Cl₂, 2-aminopyrazine, toluene, THF, 82%. (v) HCOOH, NH₃(gas), CH₃OH, 0 °C, 0.25 h, 63%. (vi) Dess–Martin periodinane, CH₂Cl₂, 25 °C, 2 h, 75%.

rat acute toxicity study with compound **1** (300 mg/kg, po single dose) and ent-**1** (600 mg/kg single dose, po) was conducted. In this experiment, a dramatic increase in serum triglycerides was

consistently noted with both compounds, with approximately 600 and 400% increases for ent-**1**- and **1**-treated rats, respectively. These data together demonstrate that both

Scheme 6. Synthesis of Piragliatin 4^a

^aReagents and conditions: (i) Pyridinium PTS, 2-cyclopetane-1-one, cyclohexane, reflux, 4 h, 92%. (ii) Et₂Zn, ICH₂Cl, 1,2-dichloroethane, -12 to 25 °C, 2.5 h, 68%. (iii) K₂CO₃, TMS-iodide, CH₂Cl₂, -8 to 25 °C, 2 h, 72%. (iv) HMDS, *n*-BuLi, THF, -20 to 0 °C, 62, 3.5 h, 65%. (v) 9 N H₂SO₄, dioxane, reflux, 72%. (vi) 0.05 M dimethyl dioxirane, acetone, 25 °C, 1 h, 90%. (vii) (COCl)₂, cat. DMF, 2-aminopyrazine, pyridine, toluene, CH₂Cl₂, 25 °C, 18 h, 43%.

Table 1. Compound 1 Metabolite Profile

| liver microsomes | % | | | | | |
|-------------------|-----|-------|-----------------|-----|------|------|
| | M1 | M2/M3 | M4 | M5 | M6 | M7 |
| CD 1 mouse | 1 | 8 | ND ^a | 2.4 | 14 | 3.1 |
| Wistar rat | 3 | 22.5 | 1.6 | 0.4 | 3.7 | 1.1 |
| beagle dog | 0.1 | 2.9 | 0 | 0.9 | 4.7 | 2.5 |
| cynomolgus monkey | 7.5 | 8.9 | 0.8 | 9.5 | 20.5 | 10.2 |
| human | 1.8 | 8 | 0.2 | 2.5 | 9.3 | 2.4 |

^aND, not detected.

Table 2. Rat Hepatic Toxicity Studies

| compd | duration (days) | dose/s (mg/kg), route, and frequency | Oil Red O stain result | glucose-lowering effect |
|-------|-----------------|--------------------------------------|------------------------|-------------------------|
| 1 | 5 | 100, po, qd | positive | + |
| ent-1 | 5 | 250, po, qd | positive | — |
| 2 | 5 | 30, 100, 300, po, qd | positive | — |
| 1 | 1 | 300, po, qd | positive | + |
| ent-1 | 1 | 600, po, qd | positive | — |

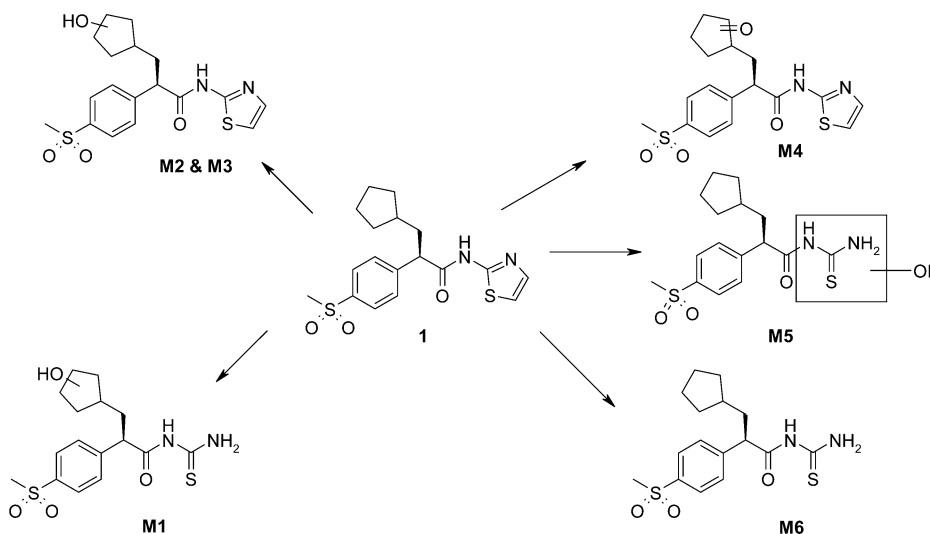


Figure 2. Metabolite profile of compound 1 in liver microsomes.

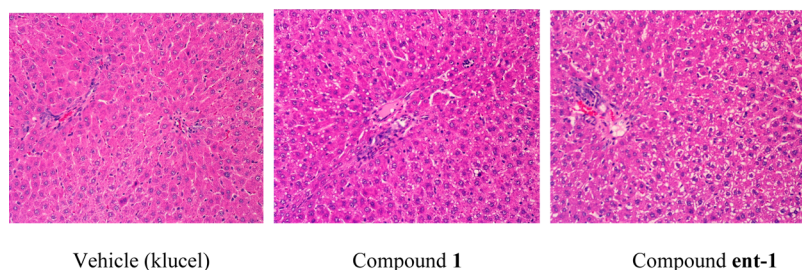


Figure 3. Oil Red O stain of liver tissue following a single dose of vehicle or compound **1** (300 mg/kg) or ent-**1** (600 mg/kg).

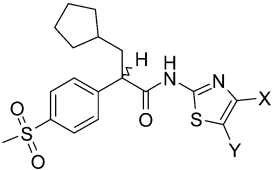
stereoisomers affected hepatobiliary function and caused hypertriglyceridemia. The hypertriglyceridemia was not accompanied by hypercholesterolemia or an increase in free fatty acids. In both compounds ent-**1**- and **1**-treated rats, periportal hepatocellular microvesicular lipidosis was noted in H&E-stained sections (see Oil Red O staining comparison, Figure 3), but only compound **1** lowered glucose levels. Taken together, these findings strongly supported the hypothesis that the thiourea metabolites formed via oxidative thiazole ring opening were the primary cause for the observed hepatic lipidosis associated with the GK activator **1**.

In an effort to identify thiazole analogues devoid of thiourea metabolite formation, several substituted thiazole analogues of **1** (Table 3) were prepared and investigated for their propensity

not form a significant amount of the thiourea metabolite, but their potency was markedly reduced. In view of suboptimal properties of these thiazole analogues of **1**, we turned our attention to alternative heterocyclic ring systems as replacements to the thiazole moiety.

Our SAR studies of the compound **1** suggested a significant “cross-talk” between the aromatic ring and the heterocyclic ring in modulating GK activity. Initially, we explored the SAR by incorporating an electron-withdrawing or an electron-donating group adjacent to the 4-methylsulfone in the aryl ring at position 3 (Table 4). In these studies, 3-chloro **12** or 3-cyano

Table 3. Metabolism of Thiazole Analogues to the Thiourea **2**

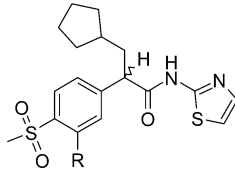


| compd | substitution | SC _{1.5} (μM) ^a | thiourea 2 concn (ng/mL) |
|-----------|---|-------------------------------------|---------------------------------|
| 1 | X, Y = H (<i>R</i> -isomer) | 0.24 ± 0.019 (25) | 505.7 |
| 5 | X = CH ₂ CH ₂ OH, Y = H | 0.667 | 167.3 |
| 6 | X = CH ₂ OH, Y = H | 0.480 | 88.7 |
| 7 | X = H, Y = Cl | 0.148 | 48.0 |
| 8 | X = H, Y = Br | 0.135 | 42.7 |
| 9 | X = H, Y = CONH ₂ | 0.734 | <10 |
| 10 | X = H, Y = CONHCH ₃ | 1.40 | <10 |
| 11 | X = H, Y = NO ₂ | 4.17 | <10 |

^aData reported as means ± SEMs (*n*). The average CV of the assay was 15%, based on an analysis of 452 compounds (SC_{1.5} < 2 μM) assayed in duplicate.

to form the thiourea metabolite **2** in incubations with human liver microsomes. Compounds **5** and **6**, the hydroxyethyl and hydroxymethyl analogues, respectively, were prepared to introduce the polar hydroxyl moiety and potentially improve the metabolic stability. These analogues were found to generate only 1/3 and 1/5 as much of thiourea metabolite as **1** but were less potent by about 3- and 2-fold, respectively, as compared to **1**. While the chloro **7** and bromo **8** analogues had ~2-fold improved potency and only about 10% of the thiourea formed as compared to **1**, they were found to have poorer pharmacokinetics (PK) properties and in vivo activity (data not shown) and therefore were abandoned. The carboxamide **9**, *N*-methylamine carboxamide **10**, and nitro **11** analogues did

Table 4. SAR of Compound **1** Analogues

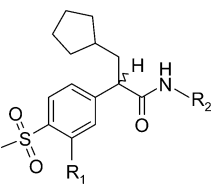


| compd | R | SC _{1.5} (μM) ^a |
|------------------------|-----------------|-------------------------------------|
| 1a ^b | H | 0.34 |
| 12 | Cl | 0.119 |
| 13 | Br | 0.111 |
| 14 | F | 0.292 |
| 15 | CF ₃ | 0.068 |
| 16 | NO ₂ | 0.065 |
| 17 | CN | 0.188 |
| 18 | NH ₂ | 0.579 |

^aData reported as means ± SEMs. The average CV of the assay was 15%, based on an analysis of 452 compounds (SC_{1.5} < 2 μM) assayed in duplicate. ^bRacemate of **1**

17 analogues were found to be about 2–3-fold more potent than **1a**, the racemate analogue corresponding to compound **1**, while the 3-fluoro **14** analogue was roughly equipotent. Other analogues containing electron-withdrawing groups such as 3-bromo **13**, 3-trifluoromethyl **15**, or 3-nitro **16** were 3–5-fold more potent in comparison to **1a**. The electron-donating 3-amino **18** was about 2-fold less potent than **1a**. Among these aromatic ring three-substituents, we chose the 3-chloro **12** analogue as a comparator to explore the SAR of various six-membered heterocycles due to its improved potency with only a modest increase in the molecular weight vs **1a**. The SAR comparing the 3-chloro and 3-*des* chloro analogues is shown in Table 5. Surprisingly, when the thiazole of **1a** was replaced by a six-membered heterocycle, such as a pyridine **19**, a pyrazine **21**, a pyrimidine **25**, or a quinoline **23**, there was about 4–5-fold loss of activity vs **1a** (SC_{1.5} values 1.21, 1.78, 1.38, and 1.74 μM vs 0.34 μM of **1a**). In a striking contrast, the corresponding 3-chloro-4-methylsulfone phenyl analogues **20**, **22**, **24**, and **26**

Table 5. Six-Membered Heteroaromatics SAR



| compd | R ₁ | R ₂ | SC _{1.5} (μM) ^a |
|-------|----------------|-------------------|-------------------------------------|
| 19 | H | 2-aminopyridine | 1.21 ± 0.49 (3) |
| 20 | Cl | 2-aminopyridine | 0.083 |
| 21 | H | 2-aminopyrazine | 1.78 |
| 22 | Cl | 2-aminopyrazine | 0.18 |
| 23 | H | 2-aminoquinoline | 1.38 |
| 24 | Cl | 2-aminoquinoline | 0.12 |
| 25 | H | 3-aminopyrimidine | 1.74 |
| 26 | Cl | 3-aminopyrimidine | 0.19 |

^aData reported as means ± SEMs (*n*). The average CV of the assay was 15%, based on an analysis of 452 compounds (SC_{1.5} < 2 μM) assayed in duplicate.

were found to have enhanced potency (SC_{1.5} values 0.083, 0.18, 0.12, and 0.15 μM, respectively) of about 9–15-fold vs the corresponding *des*-chloro analogues (19, 21, 25, and 23) (Table 5). These observations suggested significant cross-talk between the aryl group and the heterocycle and a preference for a combination of an electron-deficient aryl group with a five- or a six-membered heterocycle to obtain potent GKA activity in the phenyl acetamide series.

After extensive comparison of *in vitro*, *in vivo* potency, and rodent pharmacokinetics, followed by rat exploratory toxicity studies on select compounds, compound 3 (RO0505082) was found to have the most desirable efficacy and toxicity profile in rodents and was selected as a lead candidate for detailed profiling. Compound 3 was found to be a potent GK activator both *in vitro* (SC_{1.5}, 0.14 μM) and *in vivo*. Compound 3 was effective in reducing fasting and postprandial glucose levels,

similar to compound 1. More interestingly, in a rodent 14 day range-finding toxicity study at doses up to 600 mg/kg, there was no evidence for hepatic lipidosis (data not shown).

However, compound 3 was found to be a potent inhibitor of the hERG potassium channel (IC₂₀ < 3 μM; IC₅₀ = 7.3 μM) and increased the action duration potential in a rabbit Purkinje fiber assay (EC₅₀ at 1 Hz, 8.2 μM), suggesting a potential for cardiovascular risk based on the low margin between the plasma efficacious exposure levels and the hERG IC₂₀ values. In addition, compound 3 caused a time-dependent inhibition of CYP3A4 (54% inhibition at 24 min, 10 μM incubation), indicating a potential for drug–drug interactions and undesired nonspecific covalent modification of proteins, which could lead to unpredictable idiosyncratic toxicity. These findings posed an unacceptable risk for further development, and consequently, compound 3 was abandoned.

Detailed characterization of the metabolites of compound 3 from liver microsomal studies, *in vivo* rat PK, and safety studies showed significant formation of alcohol (M1, M2, and M4) and ketone (M3) metabolites resulting from oxidation of the cyclopentyl ring at C2 and C3 (Figure 4 and Table 6). The extent of metabolism in liver microsomal studies was found to be 76% in human and rat, while in dog it was 56%. Initially, the authentic diastereomeric mixtures of metabolites were synthesized for potency and *in vitro* safety evaluations.

The diastereomeric mixtures of the C2-hydroxyl 27 and C3-hydroxyl 28 metabolites were less potent GK activators as compared to the parent 3 (Table 7). However, the diastereomeric mixtures of C2-(29) and C3-(30) ketone metabolites retained the most potency. We chose to further evaluate the C3-ketone metabolite diastereomeric mixture 30 over the C2-keto metabolites 29 in view of the potential of the C2-ketone to promote epimerization of the adjacent chiral center. Comparison of both *R,R*-4 and *R,S*-31 diastereomers (Table 8) clearly indicated the superior potency of 4 over 31. A review of the compound profiles led to the selection of the *R,R*-diastereomer, 4, piragliatin as the clinical lead.

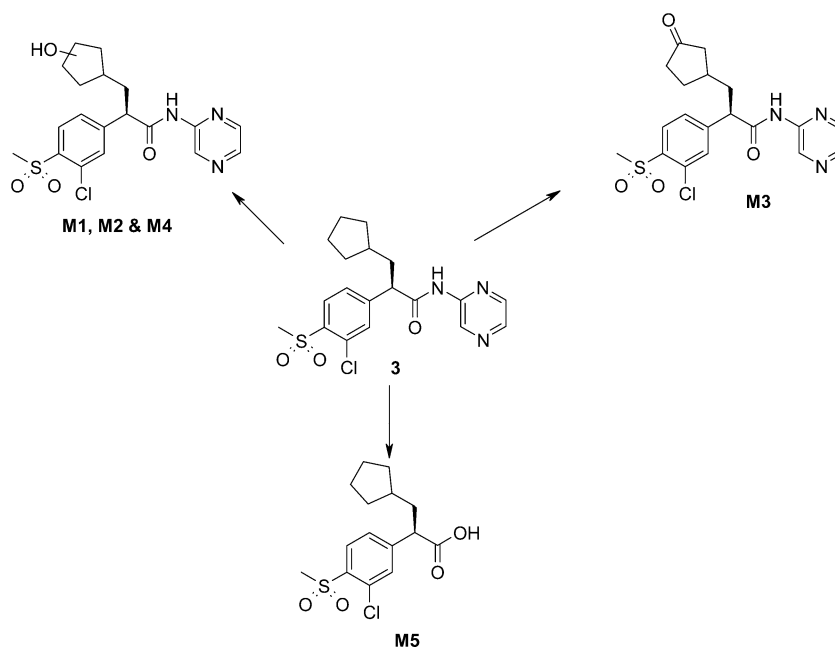
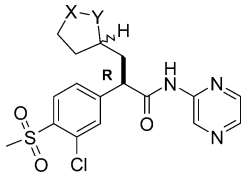


Figure 4. Metabolite profile of compound 3.

Table 6. Metabolite Profiles of Compound 3 in Rat, Mouse, Dog, Monkey, and Human Liver Microsomes

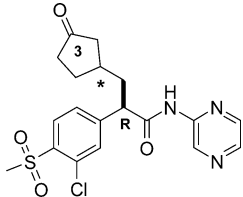
| pooled liver microsomes | % | | | | | 3 | total metabolism (%) |
|-------------------------|------|------|------|-----|-----|------|----------------------|
| | M1 | M2 | M3 | M4 | M5 | | |
| CD1 mouse | 38.4 | 16.4 | 12.3 | 1.1 | 0 | 31.9 | 68.1 |
| SD rat | 44 | 17.9 | 13.2 | 1 | 0 | 23.9 | 76.1 |
| cynomolgus monkey | 24 | 37.9 | 27.7 | 2.5 | 0 | 7.8 | 92.2 |
| beagle dog | 19.1 | 28 | 6.2 | 2.2 | 0 | 44.5 | 55.5 |
| human | 32.4 | 26.9 | 12.5 | 1.9 | 2.6 | 23.6 | 76.4 |

Table 7. In Vitro Activity of Diastereomeric Mixtures of 2,3-Hydroxyl and 2,3-Keto- Compound 3 Metabolites

|  | | | |
|---|-----------------|-----------------|-------------------------------------|
| compd | X | Y | SC _{1.5} (μM) ^a |
| 3 | CH ₂ | CH ₂ | 0.14 ± 0.039 (276) |
| 27 | CH ₂ | CHOH | 2.73 |
| 28 | CHOH | CH ₂ | 2.37 |
| 29 | CH ₂ | C=O | 0.19 |
| 30 | C=O | CH ₂ | 0.33 ± 0.048 (5) |

^aData reported as means ± SEMs (*n*). The average CV of the assay was 15%, based on an analysis of 452 compounds (SC_{1.5} < 2 μM) assayed in duplicate.

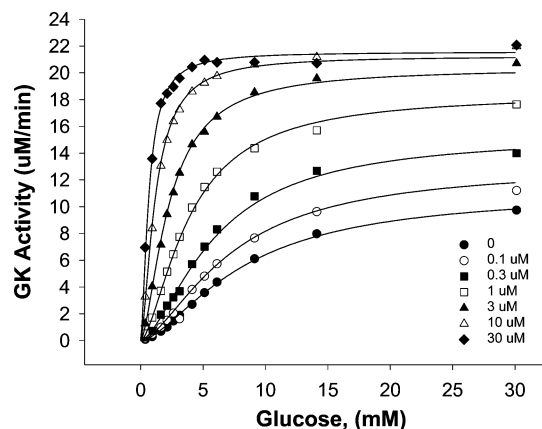
Table 8. In Vitro Activity of 3-Keto Metabolite Diastereomers of Compound 3

|  | | |
|---|----|-------------------------------------|
| compd | * | SC _{1.5} (μM) ^a |
| 31 | S- | 5.0 ± 0.81 (2) |
| 4 | R- | 0.18 ± 0.039 (9) |

^aData reported as means ± SEMs (*n*). The average CV of the assay was 15%, based on an analysis of 452 compounds (SC_{1.5} < 2 μM) assayed in duplicate.

Enzymatic assays conducted with recombinant human GK illustrated that **4** increased the enzymatic activity of GK in a dose-dependent manner at all glucose concentrations tested (Figure 5). Compound **4** at a concentration of 1 μM caused an increase in *V*_{max} of GK from 10.6 to 17.9 μM/min and decreased the *S*_{0.5} (also referred to as *K*_m for noncooperative enzyme kinetics) for glucose from 7.6 to 3.7 mM. Compound **4** increased the *V*_{max} of GK and decreased its *S*_{0.5} for glucose in a dose-dependent manner. These combined effects increased the catalytic effectiveness of GK to metabolize glucose. Activation of GK by **4** is consistent with a rate equation for a nonessential, mixed-type activator.

Compound **4** was found to have good druglike properties with good solubility, permeability, and low clearance in human hepatocytes. Compound **4** was found to have 3-fold reduced hERG IC₅₀ inhibition vs compound **3**, while in terms of IC₂₀, the improvement was only ~2 fold. Compound **4** was also

Figure 5. Effect of **4** on GK enzymatic activity.

extensively evaluated in dog telemetry studies and found to be devoid of QT prolongation (data not reported). Compound **4** did not show enzyme inhibition versus seven major CYPs, suggesting a reduced potential for drug–drug interactions. Thus, compound **4** was found to have acceptable in vitro safety properties (Table 9).

Table 9. Physical and in Vitro Safety Property Profile of Compound **4**

| property | value |
|---|-----------------------------|
| Log <i>D</i> at pH 7.4 | 1.45 |
| solubility | 0.8 mg/mL |
| Caco-2 permeability (<i>P</i> _{app}) | 1.6 × 10 ^{−6} cm/s |
| human hepatocyte clearance (<i>Cl</i> _h) | 2.2 mL/min/kg |
| human plasma protein binding | 50% |
| CYP inhibition—IC ₅₀ | >50 μM vs 7 major CYPs |
| hERG—IC ₂₀ | 5.8 μM |
| hERG—IC ₅₀ | 23.0 μM |

Pharmacokinetic and drug metabolism studies in animals showed that compound **4** was absorbed in its oral form, with the following oral bioavailability, 39% in mice and rats, 144% in dogs, and 35% in monkeys (Table 10), and volume of distribution values range was *V*_{ss} (L/kg) = 2.8–4.9. Plasma protein binding was low in all species including humans (~50%). Thus, the PK of compound **4** was characterized by high systemic plasma clearance, short to moderate elimination half-lives, and large volume of distribution in preclinical animal models.

Compound **4** was metabolized to at least five metabolites (M1–M5) before elimination (Figure 6 and Table 11). Of these, the metabolite M5 structure was not assigned. In addition, reversible metabolism of **4** was observed. The major circulating metabolite M4 was formed by a cytosolic reductase, and CYP3A4 converted M4 back to **4**. Seventy-two hours after

Table 10. Pharmacokinetic Properties of Compound 4

| species | dose (mg/kg) | route | Cl (mL/min/kg) | Vss(L/kg) | AUC _{0-inf} (ng h/mL) | C _{max} (ng/mL) | T _{max} (h) | F _{po} (%) |
|---------|--------------|-------|----------------|-----------|--------------------------------|--------------------------|----------------------|---------------------|
| mouse | 10 | iv | 111.26 | 3.332 | 1501 | 6460 | | |
| | 30 | po | | | 1765 | 1050 | 0.5 | 39 |
| | 60 | po | | | 5804 | 3750 | 1 | 65 |
| rat | 10 | iv | 103.85 | 4.975 | 1622 | 4390 | | |
| | 30 | po | | | 1885 | 404 | 2 | 39 |
| | 60 | po | | | 8253 | 2240 | 1 | 79.5 |
| dog | 10 | iv | 19.66 | 2.15 | 8830 | 8750 | | |
| | 30 | po | | | 38000 | 5228 | 2.75 | 144 |
| monkey | 5 | iv | 24.47 | 2.872 | 3416 | 3328 | | |
| | 5 | po | | | 1200 | 254 | 0.875 | 35.3 |

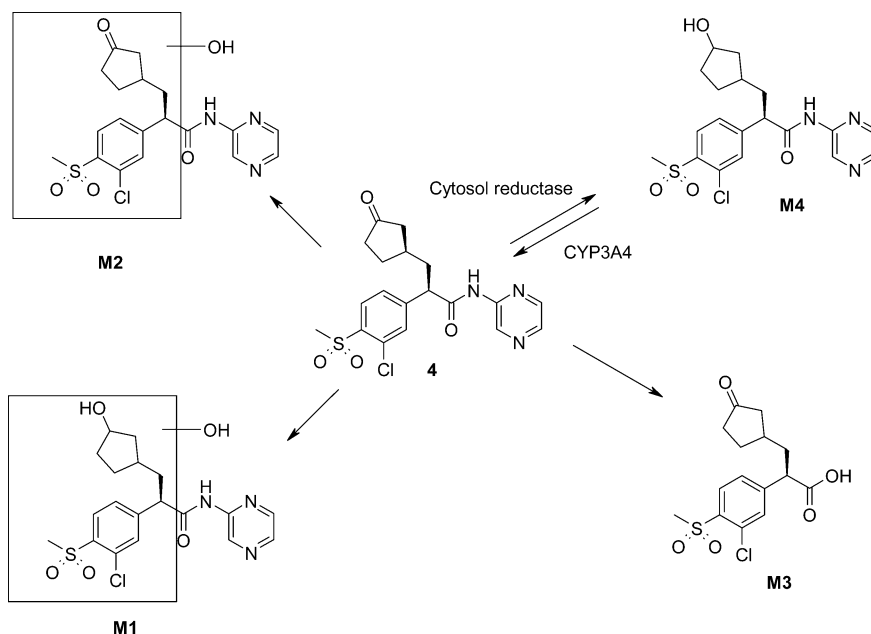


Figure 6. Metabolite profile of compound 4.

Table 11. Metabolite Profile of C¹⁴-Labeled Compound 4 in Liver Microsomes

| species ^a | % | | | | | parent | total metabolism (%) |
|----------------------|-----|------|-----|-----------------|-----|--------|----------------------|
| | M1 | M2 | M3 | M4 ^c | M5 | | |
| beagle dog | 0.3 | 7 | 1.1 | 0.2 | 1 | 90.4 | 9.6 |
| human ^b | 0.6 | 6.1 | 2 | 1.1 | 0.8 | 89.4 | 10.6 |
| cynomolgus monkey | 1.3 | 10.6 | 4.6 | 1.7 | 1.1 | 80.6 | 19.4 |
| mouse | 1.7 | 19.9 | 4.3 | 0.9 | 1.9 | 71.3 | 28.7 |
| SD rat | 0.9 | 17 | 1.7 | 0.8 | 1.4 | 78.3 | 21.7 |

^aSex, male. ^bMale and female pooled. ^cMixture of two diastereomers.

iv administration to rats, 74% of 4 was excreted in feces as metabolites, while 22% was excreted in urine as parent drug and metabolites. In vitro studies showed no significant inhibition of the human liver CYP enzymes by 4.

On the basis of its overall potency, in vitro safety assessment, and pharmacokinetic profile, compound 4 was evaluated for its glucose-lowering effect in rodents. The effect of compound 4 on postprandial glucose was tested in an oral glucose tolerance test (OGTT) study in diet-induced obese (DIO) male C57Bl/6J mice. Overnight fasted mice were dosed orally (5, 10, and 15 mg/kg) and given an oral glucose challenge (1 g/kg) 1 h

postdose. As shown in Figure 7, at all doses, significant blunting of the glucose excursion (p values <0.05 for all time points between 0 and 120 min postdose) was observed. A parallel oral PK exposure experiment with compound 4 at 5, 10, and 15 mg/kg doses was conducted. In this experiment, exposure levels of compound 4 at 60 min postdose ranged from 2.5 to 8 times over its SC_{1.5} value (0.18 μ M), explaining the robust response in the OGTT experiment. These findings suggest an improved glucose tolerance in the treatment group.

A dose–effect study in DIO mice at 5, 10, and 15 mg/kg doses by oral route was conducted with compound 4. In this study, dose-dependent decreased basal glucose levels were observed (Figure 8), with a maximal potency value of an ED₄₀ (effective dose for 40% glucose lowering vs vehicle control at 2 h postdose) value of 15.6 mg/kg and a minimal potency of ED₁₅ value at 4 h dose was 8.7 mg/kg.

Compound 4 was extensively evaluated for safety in rodent and nonrodent species. In these studies, it was found to have an acceptable therapeutic window. In a 4 week rat toxicity study (120 mg/kg, po, qd) with compound 4, exposures as high as 43000 ng h/mL did not show lipidosis (data not shown), whereas with compound 1, hepatic lipidosis was seen at all doses in a 4 week rat GLP toxicity study. Therefore, a therapeutic window for compound 1 was not established, due to lack of a no adverse effect level (NOAEL) for hepatic

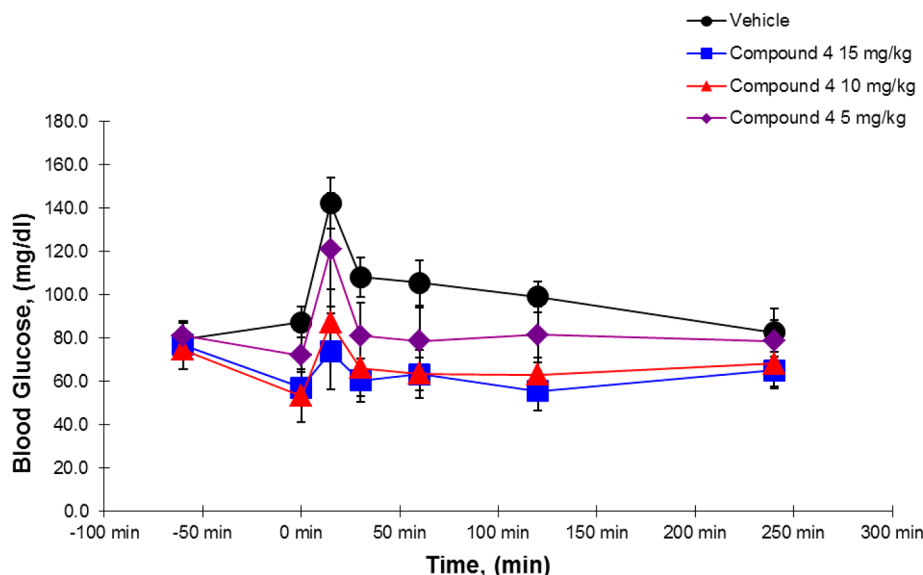


Figure 7. Compound 4 OGTT in DIO mice.

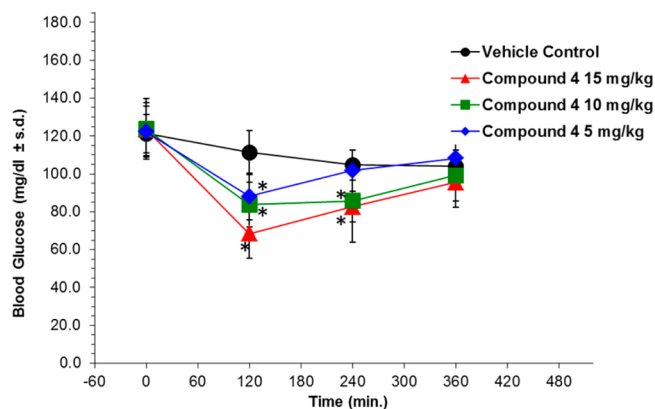


Figure 8. Compound 4 lowers basal glucose levels in DIO (* $p < 0.05$).

lipidosis. These studies strongly suggested that in rodents, hepatic lipidosis observed with compound 1 was due to its structure and not due to GK activation.

Piragliatin 4 was advanced to clinical testing. In these trials, compound 4 decreased fasting and post-OGTT glucose levels, improved the insulin secretory profile, increased β -cell sensitivity to glucose, and decreased hepatic glucose output.¹⁵ Piragliatin development was stopped because of its unfavorable risk–benefit profile observed during the phase 2 program. A third generation GKA was developed by Roche, called ROS305552, and was recently out-licensed to Hua Medicine for the treatment of T2D.¹⁶

EXPERIMENTAL SECTION

Chemistry. All nonaqueous reactions were carried out under an argon or nitrogen atmosphere at 25 °C, unless otherwise noted. All reagents and anhydrous solvents were used as obtained commercially without further purification or distillation, unless otherwise stated. Analytical thin-layer chromatography (TLC) was performed on EMD Chemicals silica gel 60 F254 precoated plates (0.25 mm). Compounds were visualized by UV light and/or stained with either *p*-anisaldehyde, iodine, or phosphomolybdic acid or KMnO_4 solutions followed by heating. Analytical high-pressure liquid chromatography (HPLC) and LC-MS analyses were conducted using the following two instruments and conditions. Method 1: Hewlett-Packard HP-1090 pump and HP-

1090 PDA detector set at 215 nm with the MS detection performed with a Micromass Platform II mass spectrometer with electrospray ionization (ESI); Chromegabond WR C18 3 μm , 120 Å, 3.2 mm \times 30 mm column; solvent A, H_2O –0.02% TFA; solvent B, MeCN–0.02% TFA; flow rate, 2 mL/min; start 2% B, final 98% B in 4 min, linear gradient. Method 2: Waters 2795 pump and Waters 2996 photodiode array detector set at 214 nm with the MS detection performed with a Waters ZQ mass spectrometer (ESI); Epic Polar Hydrophilic 3 μm , 120 Å, 3.2 mm \times 30 mm column; solvent A, H_2O –0.03% HCO_2H ; solvent B, MeCN–0.03% HCO_2H ; flow rate, 2 mL/min; start 10% B, final 100% B in 3 min linear gradient, remaining for 1 min. Compounds were purified using either of the following methods. Flash column chromatography was performed on EM Science silica gel 60 (particle size of 32–63 μm , 60 Å). Preparative reverse-phase high-pressure liquid chromatography (RP-HPLC) used a Waters Delta prep 4000 pump/controller, a 486 detector set at 215 nm, and a LKB Ultrarac fraction collector. The sample was dissolved in a mixture of MeCN/20 mM aqueous NH_4Ac , applied on a C-18 20 mm \times 100 mm column, and eluted at 30 mL/min with a 20 min linear gradient of 10–90% B, where solvent A was H_2O with 20 mM NH_4Ac and solvent B was MeCN. The pooled fractions were concentrated under reduced pressure and lyophilized to afford the desired compounds. All compounds reported herein are analyzed in one of the two analytical HPLC methods described above and possess purity of at least 95%. ^1H NMR spectra were recorded using a Varian Mercury 300 MHz or Varian Inova 400 MHz spectrometer. The chemical shifts are in parts per million (δ) referenced to Me_4Si (0.00 ppm) or CHCl_3 (7.26 ppm). High-resolution mass spectra (HRMS) were recorded on a Bruker Apex II FTICR mass spectrometers with a 4.7 T magnet (ES) or Micromass AutoSpec (EI) mass spectrometers.

(3-Chloro-4-methylsulfanyl-phenyl)-oxo-acetic Acid Methyl Ester (37b). A solution of anhydrous aluminum chloride (54.9 g, 412 mmol) in chloroform (180 mL) under argon was cooled to 0 °C and then treated dropwise with a solution of methyl chloroacetate (24.3 mL, 264 mmol) in chloroform (180 mL). The resulting reaction mixture was stirred at 0 °C for an additional 30 min and then treated dropwise with a solution of 2-chlorothioanisole 36 (39.4 g, 247 mmol) in chloroform (180 mL). The solution turned red in color. The resulting reaction mixture was allowed to warm to 25 °C, where it was stirred for 4 h. The reaction mixture was then slowly poured onto ice (700 mL). The resulting yellow mixture was stirred for 15 min and filtered through Celite to remove aluminum salts. The filtrate was extracted with methylene chloride (3 \times 50 mL). The combined organic layers were washed with saturated aqueous sodium carbonate solution (1 \times 50 mL). The organic layer was dried over magnesium sulfate, filtered,

and concentrated in vacuo to afford (3-chloro-4-methylsulfanyl-phenyl)-oxo-acetic acid methyl ester **37b** (4.32 g, 65.3%) as a light yellow oil. EI-HRMS m/e calcd for $C_{10}H_9ClSO_3$ (M^+), 243.09961; found, 243.9958. 1H NMR (300 MHz, chloroform- d): δ 8.02 (d, J = 1.83 Hz, 1H), 7.94 (dd, J = 1.65, 8.24 Hz, 1H), 7.23 (d, J = 8.42 Hz, 1H), 3.99 (s, 3H), 2.55 (s, 3H).

(3-Chloro-4-methylsulfanyl-phenyl)-oxo-acetic Acid (**60**). (3-Chloro-4-methylsulfanyl-phenyl)-oxo-acetic acid methyl ester (61.7 g, 252 mmol) in toluene (120 mL) was heated at 50 °C. This heated solution was treated dropwise with a 3 M aqueous sodium hydroxide solution (105 mL, 313 mmol) via a dropping funnel, taking care to keep temperature below 60 °C. After the addition was complete, the reaction mixture was stirred at 50 °C for 1.5 h, during which time a yellow precipitate began to form. After this time, the heat was removed, and the warm solution was treated dropwise with concentrated hydrochloric acid (10.6 mL, 290 mmol). The resulting reaction mixture was cooled to 25 °C and then was stirred at 25 °C for 16 h. The solid was filtered and then washed with water (50 mL) and toluene (50 mL). The solid was dried by suction for 1 h and then dried in a high vacuum desiccator to afford (3-chloro-4-methylsulfanyl-phenyl)-oxo-acetic acid **60** (57.22 g, 98%) as a white solid; mp 166° (dec). FAB-HRMS m/e calcd for $C_9H_7ClO_3S$ ($M + H$) $^+$, 252.9702; found, 252.9700. 1H NMR (300 MHz, DMSO- d_6): δ 7.76–7.84 (m, 2H), 7.44 (d, J = 8.06 Hz, 1H), 2.57 (s, 3H).

(3-Chloro-4-methylsulfanyl-phenyl)-acetic Acid (**61**). A reaction flask equipped with a mechanical stirrer was charged with hydrazine hydrate (8.5 mL, 273 mmol). The hydrazine hydrate was cooled to –50 °C and then treated with (3-chloro-4-methylsulfanyl-phenyl)-oxo-acetic acid **60** (12.6 g, 54.6 mmol) in one portion. An exotherm ensued that raised the temperature. The resulting white mixture was then heated to 80 °C. After it reached 80 °C, the heating element was removed, and the reaction mixture was treated with potassium hydroxide (2.09 g, 31.7 mmol) in one portion. An exotherm was observed. The reaction mixture was allowed to cool back to 80 °C. This potassium hydroxide addition process was repeated three times (3 \times 2.09 g). At the end of the final potassium hydroxide portion addition, the reaction mixture was heated to 100 °C for 16 h. The resulting homogeneous reaction mixture was cooled to 25 °C and then diluted with water (12 mL). The reaction mixture was then transferred to separatory funnel, rinsing with additional water (12 mL) and diethyl ether (40 mL). The layers were separated, and the aqueous layer was transferred to a flask. The organic layer was extracted with water (2 \times 15 mL). The aqueous layers were combined and treated with heptane (20 mL), and the resulting reaction mixture was vigorously stirred. This stirred reaction mixture was treated with dropwise with concentrated hydrochloric acid (26 mL) over 30 min, while the temperature was kept under 50 °C with an ice bath. A cloudy suspension was formed, and this suspension was stirred at 25 °C for 3 h. The solid that formed was filtered and washed sequentially 1 N hydrochloric acid (2 \times 6 mL), heptane (1 \times 12 mL), and a solution of heptane/diethyl ether (15 mL, 4:1). The resulting solid was dried under high vacuum to afford (3-chloro-4-methylsulfanyl-phenyl)-acetic acid **61** (10.48 g, 89%) as an off-white solid; mp 105.6–108.4 °C. EI-HRMS m/e calcd for $C_9H_9ClO_2S$ (M^+), 216.0012; found, 216.0022. 1H NMR (300 MHz, chloroform- d): δ 7.30 (d, J = 1.10 Hz, 1H), 7.16–7.21 (m, 1H), 7.11–7.16 (m, 1H), 3.61 (s, 2H), 2.48 (s, 3H).

(3-Chloro-4-methylsulfanyl-phenyl)- N -[2(R)-hydroxy-1(R)-methyl-2(R)-phenyl-ethyl]- N -methyl-acetamide (**62**). A mixture of (3-chloro-4-methylsulfanyl-phenyl)-acetic acid **61** (10.48 g, 48.4 mmol) and potassium carbonate (20.1 g, 145.1 mmol) in acetone (65 mL) was cooled to –10 °C. The pale yellow was then treated dropwise with trimethyl acetylchloride (6.25 mL, 50.8 mmol) while maintaining the temperature below –10 °C. The resulting reaction mixture was stirred at –10 °C for 10 min and then allowed to warm to 0 °C, where it was stirred for 10 min. The reaction mixture was recooled to –10 °C and then treated with (1*R*,2*R*)-(-)-pseudoephedrine (11.99 g, 72.5 mmol), resulting in an exotherm. The reaction mixture was stirred at –10 °C for 10 min and then warmed to 25 °C, where it was stirred for 1 h. The reaction mixture was quenched with water (50 mL) and then extracted with ethyl acetate (1 \times 100 mL). The organic layer was

washed with water (2 \times 40 mL). The combined aqueous layer was back-extracted with ethyl acetate (2 \times 50 mL). The combined organic layer was dried over magnesium sulfate, filtered, and concentrated in vacuo. The crude material was recrystallized from ethyl acetate (45 mL) and hexanes (80 mL) to afford (3-chloro-4-methylsulfanyl-phenyl)- N -[2(R)-hydroxy-1(R)-methyl-2(R)-phenyl-ethyl]- N -methyl-acetamide **62** (13.75 g, 78%) as a light yellow solid; mp 111.5–112.9 °C; $[\alpha]_{589}^{23}$ = –97.2° (c 0.104, chloroform). FAB-HRMS m/e calcd for $C_{19}H_{22}ClNO_2S$ ($M + H$) $^+$, 364.1138; found, 364.1142. 1H NMR (300 MHz, chloroform- d): δ 6.98–7.57 (m, 8H), 4.54–4.67 (m, 1H), 4.02, 4.50 (2s, 1H), 3.63, 3.75 (2s, 2H), 2.84, 2.97 (2m, 3H), 2.39–2.54 (m, 3H), 0.92, 1.14 (2d, J = 6.6 Hz, 3H).

2(R)-(3-Chloro-4-methylsulfanyl-phenyl)-3-cyclopentyl- N -[2(R)-hydroxy-1(R)-methyl-2(R)-phenyl-ethyl]- N -methyl-propionamide (**63**). A solution of 1,1,1,3,3,3-hexamethyldisilazane (17.9 mL, 85 mmol) in tetrahydrofuran (90 mL) was cooled to –78 °C and then treated with a 2.34 M solution of n -butyl lithium in hexanes (33.9 mL, 79.3 mmol). The reaction mixture was stirred at –78 °C for 15 min and then treated with (3-chloro-4-methylsulfanyl-phenyl)- N -[2(R)-hydroxy-1(R)-methyl-2(R)-phenyl-ethyl]- N -methyl-acetamide **62** (13.75 g, 37.8 mmol) in tetrahydrofuran (90 mL), while maintaining the temperature below –65 °C. The resulting yellow-orange solution was stirred at –78 °C for 15 min and then allowed to warm up to 0 °C, where it was stirred for 20 min. The reaction mixture was then recooled to –78 °C and treated with iodomethyl cyclopentane (11.9 g, 56.7 mmol) in 1,3-dimethyl-3,4,5,6-tetrahydro-2(1*H*)-pyrimidinone (9.6 mL, 79.3 mmol). The resulting solution was stirred at –78 °C for 30 min and then allowed to warm to 25 °C, where it was stirred for 16 h. The reaction mixture was diluted with ethyl acetate (200 mL) and then washed with aqueous ammonium chloride (1 \times 100 mL). The aqueous layer was extracted with ethyl acetate (2 \times 50 mL). The combined organic layer was washed with aqueous sodium chloride solution, dried over sodium sulfate, filtered, and concentrated in vacuo. The resulting material was redissolved in ethyl acetate and washed with 10% sulfuric acid (2 \times 100 mL) and saturated sodium bicarbonate (2 \times 100 mL), dried over magnesium sulfate, filtered, and concentrated in vacuo. The crude material was recrystallized from ethyl acetate/hexanes to afford 2(R)-(3-chloro-4-methylsulfanyl-phenyl)-3-cyclopentyl- N -[2(R)-hydroxy-1(R)-methyl-2(R)-phenyl-ethyl]- N -methyl-propionamide **63** (11.36 g, 67%) as a light yellow solid; mp 113.8–117.6 °C; $[\alpha]_{589}^{23}$ = –100.3° (c 0.049, chloroform). FAB-HRMS m/e calcd for $C_{25}H_{32}ClNO_2S$ ($M - H$) $^+$, 444.1764; found, 444.1765. 1H NMR (300 MHz, chloroform- d): δ 6.98–7.49 (m, 8H), 4.57 (m, 1H), 4.37 (br. s., 1H), 3.57, 3.97 (2m, 1H), 2.74, 2.90 (2s, 3H), 2.37–2.52 (m, 3H), 1.97–2.14 (m, 1H), 1.37–1.88 (m, 8H), 0.62, 1.14 (2d, J = 6.6 Hz, 3H), 0.97–1.15 (m, 2H).

2(R)-(3-Chloro-4-methylsulfanyl-phenyl)-3-cyclopentyl-propionic Acid (**64**). A solution of 2(R)-(3-chloro-4-methylsulfanyl-phenyl)-3-cyclopentyl- N -[2(R)-hydroxy-1(R)-methyl-2(R)-phenyl-ethyl]- N -methyl-propionamide **63** (11.36 g, 25.5 mmol) in dioxane (45 mL) was treated with 9 N aqueous sulfuric acid solution (28 mL). The resulting reaction mixture was heated at 105 °C for 16 h. The reaction was then cooled to 0 °C using an ice bath, and the product was then precipitated using the addition of water (200 mL). The suspension was stirred at 0 °C until the supernatant, which was turbid initially, became clear and light yellow in color. The solid was filtered off and dried in vacuo. The solid material was dissolved in hot glacial acetic acid (15 mL) and treated with water (10 mL) to initiate crystallization. The mixture was cooled to 25 °C and then treated with an additional amount of water (20 mL). After it was stirred at 25 °C for 1 h, the solid was collected by filtration. The solid was dried in a high vacuum desiccator with phosphorus pentoxide to afford 2(R)-(3-chloro-4-methylsulfanyl-phenyl)-3-cyclopentyl-propionic acid **64** (7.46 g, 98%) as a white solid; mp 116.9–119.2 °C; $[\alpha]_{589}^{23}$ = –55.8° (c 0.104, chloroform). EI-HRMS m/e calcd for $C_{15}H_{19}ClO_2S$ (M) $^+$, 298.0794; found, 298.0804. 1H NMR (300 MHz, chloroform- d): δ 7.34 (d, J = 1.83 Hz, 1H), 7.18–7.26 (m, 1H), 7.07–7.16 (m, 1H), 3.55 (t, J = 7.69 Hz, 1H), 2.47 (s, 3H), 1.97–2.15 (m, 1H), 1.38–1.91 (m, 8H), 0.97–1.22 (m, 2H).

2(R)-(3-Chloro-4-methylsulfonyl-phenyl)-3-cyclopentyl-propionic Acid (65). A slurry of 2(R)-(3-chloro-4-methylsulfonyl-phenyl)-3-cyclopentyl-propionic acid **64** (15.68 g, 52.5 mmol) in formic acid (10 mL) was cooled to 0 °C and then treated with 30% aqueous hydrogen peroxide solution (30 mL). The resulting reaction mixture was allowed to warm to 25 °C, where it was stirred for 16 h. The product was precipitated by the addition of water (120 mL). The solid was filtered off, washed with water, and dried by suction. Flash chromatography (Merck silica gel 60, 230–400 mesh, 50/50 hexanes/ethyl acetate plus 1% acetic acid) afforded 2(R)-(3-chloro-4-methylsulfonyl-phenyl)-3-cyclopentyl-propionic acid **65** (13.93 g, 80%) as a white solid; mp 123.9–126.2 °C; $[\alpha]_{589}^{23} = -41.5^\circ$ (c 0.176, chloroform). FAB-HRMS m/e calcd for $C_{15}H_{19}ClO_4S$ ($M+H$)⁺, 331.0771; found, 331.0776. ¹H NMR (300 MHz, chloroform-*d*): δ 8.11 (d, $J = 8.06$ Hz, 1H), 7.55 (s, 1H), 7.44 (d, $J = 8.42$ Hz, 1H), 3.69 (t, $J = 7.69$ Hz, 1H), 3.28 (s, 3H), 2.02–2.19 (m, 1H), 1.41–1.93 (m, 8H), 1.01–1.22 (m, 2H).

2(R)-(3-Chloro-4-methylsulfonyl-phenyl)-3-cyclopentyl-N-pyrazin-2-yl-propionamide (3). A solution of 2(R)-(3-chloro-4-methylsulfonyl-phenyl)-3-cyclopentyl-propionic acid **65** (200 mg, 0.61 mmol) in methylene chloride (5 mL) was treated with *N,N'*-dimethylformamide (1 drop) and then cooled to 0 °C. The reaction mixture was then treated dropwise with a 2 M solution of oxalyl chloride in methylene chloride (0.45 mL, 0.91 mmol) and stirred at 0 °C for 10 min. The reaction mixture was then treated with a solution of 2-aminopyrazine (115 mg, 1.21 mmol) and pyridine (0.245 mL, 3.03 mmol) in anhydrous tetrahydrofuran (10 mL). The resulting reaction mixture was allowed to warm to 25 °C, where it was stirred for 16 h. The reaction mixture was diluted with water (10 mL) and extracted with methylene chloride (3 \times 15 mL). The combined organic layers were dried over sodium sulfate, filtered, and concentrated in vacuo. Biotage chromatography (FLASH 40S, Silica, 50/50 hexanes/ethyl acetate) afforded 2(R)-(3-chloro-4-methylsulfonyl-phenyl)-3-cyclopentyl-N-pyrazin-2-yl-propionamide **3** (172 mg, 70%) as a white foam. EI-HRMS m/e calcd for $C_{19}H_{22}ClN_3O_3S$ (M^+), 407.1070; found, 407.1068. ¹H NMR (300 MHz, chloroform-*d*): δ 9.53 (br. s., 1H), 8.38 (br. s., 1H), 8.24 (br. s., 1H), 8.14 (d, $J = 8.42$ Hz, 1H), 7.92 (br. s., 1H), 7.63 (s, 1H), 7.50 (d, $J = 8.42$ Hz, 1H), 3.66 (t, $J = 7.51$ Hz, 1H), 3.28 (s, 3H), 2.24 (td, $J = 7.19, 13.83$ Hz, 1H), 1.39–2.02 (m, 8H), 1.16 (d, $J = 3.30$ Hz, 2H).

2-Hydroxy-cyclopentanecarboxylic Acid Ethyl Ester (66). A solution of 2-oxo-cyclopentanecarboxylic acid ethyl ester (10 g, 64.0 mmol) in ethanol (106.7 mL) cooled to 0 °C was treated with 98% sodium borohydride (686 mg, 17.78 mmol). The reaction mixture was stirred at 0 °C for 30 min. At this time, the reaction mixture was poured into water (53 mL) and was extracted into diethyl ether (3 \times 100 mL). The organics were dried over sodium sulfate, filtered, and concentrated in vacuo. Flash chromatography (Merck silica gel 60, 230–400 mesh, 75/25 ethyl acetate/hexanes) afforded 2-hydroxy-cyclopentanecarboxylic acid ethyl ester **66** (8.5 g, 83.9%) as a clear liquid. ¹H NMR (300 MHz, chloroform-*d*): δ 1.21–1.30 (m, 3 H), 1.49–2.12 (m, 6 H), 2.52–2.79 (m, 1 H), 4.05–4.16 (m, 2 H), 4.29–4.54 (m, 1 H).

2-(Tetrahydropyran-2-yloxy)-cyclopentanecarboxylic Acid Ethyl Ester (67). A solution of 2-hydroxy-cyclopentanecarboxylic acid ethyl ester **66** (3.5 g, 22.12 mmol) in methylene chloride (147.5 mL) was treated with 3,4-dihydro-2H-pyran (3.03 mL, 33.1 mmol) and pyridinium *p*-toluenesulfonate (556 mg, 2.21 mmol). This solution was stirred at 25 °C for 5 h. The reaction was washed with half-saturated aqueous sodium chloride solution (2 \times 75 mL), dried over sodium sulfate, filtered, and concentrated in vacuo. Flash chromatography (Merck silica gel 60, 230–400 mesh, 90/10 hexanes/ethyl acetate) afforded 2-(tetrahydropyran-2-yloxy)-cyclopentanecarboxylic acid ethyl ester **67** (4.7 g, 87.7%) as a clear liquid. EI-HRMS m/e calcd for $C_{13}H_{22}O$ (M^+), 242.1518; found, 242.1521. ¹H NMR (300 MHz, chloroform-*d*): δ 1.11–1.39 (m, 5 H), 1.41–2.31 (m, 10 H), 2.63–2.98 (m, 1 H), 3.36–3.63 (m, 1 H), 3.75–3.97 (m, 1 H), 4.00–4.29 (m, 2 H), 4.32–4.56 (m, 1 H), 4.59–4.83 (m, 1 H).

[2-(Tetrahydropyran-2-yloxy)-cyclopentyl]-methanol (68). A slurry of lithium aluminum hydride (883 mg, 23.27 mmol) in tetrahydrofuran (19.4 mL) cooled to 0 °C was treated with 2-

(tetrahydropyran-2-yloxy)-cyclopentanecarboxylic acid ethyl ester **67** (4.7 g, 19.59 mmol). The reaction mixture was stirred at 25 °C for 18 h. At this time, the reaction mixture was poured onto ice/water. The mixture was filtered through a pad of Celite (methylene chloride as eluent). The organics were washed with a saturated aqueous sodium chloride solution (1 \times 100 mL), dried over sodium sulfate, filtered, and concentrated in vacuo to give [2-(tetrahydropyran-2-yloxy)-cyclopentyl]-methanol **68** (3.25 g, 83.6%) as a clear liquid. EI-HRMS m/e calcd for $C_{11}H_{20}O_3$ (M^+), 200.1412; found, 200.1412. ¹H NMR (300 MHz, chloroform-*d*): δ 1.05–1.30 (m, 2 H), 1.34–2.01 (m, 12 H), 2.02–2.76 (m, 2 H), 3.37–4.09 (m, 3 H), 4.11–4.81 (m, 1 H).

2-(2-Iodomethyl-cyclopentyl)-tetrahydropyran (69). A solution of triphenylphosphine (1.70 g, 6.49 mmol) and imidazole (884 mg, 12.98 mmol) in methylene chloride (8.32 mL) cooled to 0 °C was treated with iodine (1.64 g, 6.49 mmol). After iodine was completely dissolved, a solution of 2-(tetrahydropyran-2-yloxy)-cyclopentyl]-methanol **68** (1.0 g, 4.99 mmol) was added to the reaction mixture. The reaction was stirred at 0 °C for 1 h and 25 °C for 2 h. At this time, the reaction mixture was poured into water (100 mL) and extracted with methylene chloride (1 \times 30 mL). The organics were washed with aqueous sodium thiosulfate solution (1 \times 50 mL), dried over sodium sulfate, filtered, and concentrated in vacuo at 25 °C. Flash chromatography (Merck silica gel 60, 230–400 mesh, 80/20 hexanes/ethyl acetate) afforded 2-(2-iodomethyl-cyclopentyl)-tetrahydropyran **69** (1.17 g, 75.8%) as a clear liquid. EI-HRMS m/e calcd for $C_{11}H_{19}IO_2$ (M^+), 309.0352; found, 309.0348. ¹H NMR (300 MHz, chloroform-*d*): δ 1.08–2.17 (m, 12 H), 3.10–3.36 (m, 2 H), 3.47–3.57 (m, 1 H), 3.81–3.96 (m, 2 H), 4.56–4.79 (m, 2 H).

3-Iodomethyl-cyclopentanol (71). A solution of 3-iodomethyl-cyclopentanone **70** (12.84 g, 57.31 mmol) (ref 10) in methanol (143 mL) was cooled to 0 °C and then slowly treated with sodium borohydride powder (2.38 g, 63.04 mmol). The resulting reaction mixture was stirred at 0 °C for 40 min and then slowly quenched with water (100 mL). The reaction mixture was then concentrated in vacuo to remove methanol. The resulting aqueous residue was extracted with diethyl ether (3 \times 100 mL). The combined organic extracts were dried over magnesium sulfate, filtered, and concentrated in vacuo. Flash chromatography (Merck silica gel 60, 70–230 mesh, 100% methylene chloride) afforded 3-iodomethyl-cyclopentanol **71** (7.71 g, 59%) as a green liquid. EI-HRMS m/e calcd for $C_6H_{11}IO$ (M^+), 225.9855; found, 225.9856. ¹H NMR (400 MHz, chloroform-*d*): δ 1.20–2.56 (m, 7 H), 3.21–3.35 (m, 2 H), 4.34–4.51 (m, 1 H).

2-(3-Iodomethyl-cyclopentyl)-tetrahydropyran (72). A solution of 3-iodomethyl-cyclopentanol **71** (7.71 g, 34.10 mmol) in methylene chloride (171 mL) was treated with 3,4-dihydro-2H-pyran (4.7 mL, 51.16 mmol) and pyridinium *p*-toluenesulfonate (857.1 mg, 3.41 mmol). This solution was stirred at 25 °C for 24 h. The combined organic extracts were dried over magnesium sulfate, filtered, and concentrated in vacuo. Flash chromatography (Merck silica gel 60, 70–230 mesh, 19/1 petroleum ether/diethyl ether) afforded 2-(3-iodomethyl-cyclopentyl)-tetrahydropyran **72** (7.91 g, 75%) as a yellow oil. EI-HRMS m/e calcd for $C_{11}H_{19}IO_2$ (M^+), 310.0430; found, 310.0433. ¹H NMR (400 MHz, chloroform-*d*): δ 1.09–2.52 (m, 13 H), 3.13–3.37 (m, 2 H), 3.40–3.60 (m, 1 H), 3.80–3.99 (m, 1 H), 4.24–4.42 (m, 1 H), 4.60 (d, $J = 3.30$ Hz, 1 H).

2(R)-(3-Chloro-4-methylsulfonyl-phenyl)-N-[2(R)-hydroxy-1(R)-methyl-2(R)-phenyl-ethyl]-N-methyl-3-[2-(tetrahydropyran-2-yloxy)-cyclopentyl]-propionamide (73). A solution of 1,1,1,3,3,3-hexamethylidisilazane (14.5 mL, 68.7 mmol) in tetrahydrofuran (45.8 mL) was cooled to –45 °C and then treated with 2.34 M solution of *n*-butyl lithium in hexanes (25.8 mL, 63.2 mmol). The reaction mixture was stirred at –45 °C for 30 min. At this time, it was treated with (3-chloro-4-methylsulfonyl-phenyl)-N-[2(R)-hydroxy-1(R)-methyl-2(R)-phenyl-ethyl]-N-methyl-acetamide **62** (10.0 g, 27.48 mmol) in tetrahydrofuran (46 mL). Upon complete addition, the reaction mixture was warmed to 0 °C and stirred at 0 °C for 30 min. At this time, the reaction mixture was recooled to –45 °C and then was treated with 2-(2-iodomethyl-cyclopentyl)-tetrahydropyran **69** (12.8, 41.22 mmol) in 1,3-dimethyl-3,4,5,6-tetrahydro-2(1H)-pyrimidinone (8.4 mL). The resulting solution was warmed to 0 °C, where it

was stirred for 3 h. At this time, the reaction mixture was diluted with aqueous sodium chloride solution (100 mL). The phases were partitioned. The aqueous layer was extracted with ethyl acetate (3 × 50 mL). The combined organics were washed with aqueous 10% hydrochloric acid and sodium carbonate solution, dried over sodium sulfate, filtered, and concentrated in vacuo. Flash chromatography (Merck silica gel 60, 230–400 mesh, 75/25 ethyl acetate/hexanes) afforded 2(R)-(3-chloro-4-methylsulfanyl-phenyl)-N-[2(R)-hydroxy-1(R)-methyl-2(R)-phenyl-ethyl]-N-methyl-3-[2-(tetrahydropyran-2-yloxy)-cyclopentyl]-propionamide **73** (10.6 g, 70.6%) as a yellow foam. EI-HRMS *m/e* calcd for C₃₀H₄₀ClNO₄S (M + Na)⁺, 568.2259; found, 568.2262. ¹H NMR (300 MHz, chloroform-*d*): δ 0.44–1.21 (m, 4 H), 1.31–2.28 (m, 14 H), 2.30–2.56 (m, 3 H), 2.60–3.01 (m, 4 H), 3.28–5.00 (m, 7 H), 6.95–7.59 (m, 8 H).

2(R)-(3-Chloro-4-methylsulfanyl-phenyl)-3-(2-hydroxy-cyclopentyl)-N-[2(R)-hydroxy-1(R)-methyl-2(R)-phenyl-ethyl]-N-methyl-propionamide (**74**). A solution of 2(R)-(3-chloro-4-methylsulfanyl-phenyl)-N-[2(R)-hydroxy-1(R)-methyl-2(R)-phenyl-ethyl]-N-methyl-3-[2-(tetrahydropyran-2-yloxy)-cyclopentyl]-propionamide **73** (1.04 g, 1.91 mmol) in ethanol (19.1 mL) was treated with pyridinium *p*-toluenesulfonate (48 mg, 0.19 mmol). The resulting solution was heated to 55 °C for 2 h. At this time, the reaction mixture was concentrated in vacuo. Flash chromatography (Merck silica gel 60, 230–400 mesh, 75/25 ethyl acetate/hexanes) afforded 2(R)-(3-chloro-4-methylsulfanyl-phenyl)-3-(2-hydroxy-cyclopentyl)-N-[2(R)-hydroxy-1(R)-methyl-2(R)-phenyl-ethyl]-N-methyl-propionamide **74** (0.82 g, 93%) as a white foam. EI-HRMS *m/e* calcd for C₂₅H₃₂ClNO₃S (M + Na)⁺, 484.1684; found, 484.1674. ¹H NMR (300 MHz, chloroform-*d*): δ 0.51–2.38 (m, 12 H), 2.45 (d, *J* = 8.42 Hz, 3 H), 2.63–3.01 (m, 3 H), 3.30–4.87 (m, 6 H), 6.89–7.60 (m, 8 H).

2(R)-(3-Chloro-4-methylsulfanyl-phenyl)-N-methyl-N-[1(R)-methyl-2-oxo-2(R)-phenyl-ethyl]-3-(2-oxo-cyclopentyl)-propionamide (**75**). A mixture of 2(R)-(3-chloro-4-methylsulfanyl-phenyl)-3-(2-hydroxy-cyclopentyl)-N-[2(R)-hydroxy-1(R)-methyl-2(R)-phenyl-ethyl]-N-methyl-propionamide **74** (3.63 g, 7.85 mmol), *N*-methyl-morpholine-*N*-oxide (2.76 g, 23.5 mmol), and powdered molecular sieves (7.85 g) in methylene chloride (15.7 mL) at 25 °C treated with tetrapropylammonium perruthenate (276 mg, 0.78 mmol). The resulting reaction mixture was stirred at 25 °C for 20 min. At this time, the reaction mixture was filtered through a pad of silica (ethyl acetate as eluent). The filtrate was concentrated in vacuo. Flash chromatography (Merck silica gel 60, 230–400 mesh, 75/25 ethyl acetate/hexanes) afforded 2(R)-(3-chloro-4-methylsulfanyl-phenyl)-N-methyl-N-[1(R)-methyl-2-oxo-2(R)-phenyl-ethyl]-3-(2-oxo-cyclopentyl)-propionamide **75** (2.75 g, 76.5%) as a white foam. EI-HRMS *m/e* calcd for C₂₅H₂₈ClNO₃S (M)⁺, 457.1478; found, 457.1489. ¹H NMR (300 MHz, chloroform-*d*): δ 1.36 (dd, *J* = 6.96, 3.66 Hz, 1 H), 1.43–2.56 (m, 11 H), 2.68–2.87 (m, 4 H), 4.14–4.32 (m, 1 H), 5.76–6.14 (m, 1 H), 6.89–6.97 (m, 1 H), 6.99–7.11 (m, 1 H), 7.24 (dd, *J* = 6.04, 2.01 Hz, 1 H), 7.27–7.35 (m, 2 H), 7.42–7.53 (m, 1 H), 7.69–7.86 (m, 2 H).

2(R)-(3-Chloro-4-methylsulfanyl-phenyl)-3-(2-oxo-cyclopentyl)-propionic Acid (**76**). A solution of 2(R)-(3-chloro-4-methylsulfanyl-phenyl)-N-methyl-N-[1(R)-methyl-2-oxo-2(R)-phenyl-ethyl]-3-(2-oxo-cyclopentyl)-propionamide **75** (2.75 g, 6.0 mmol) in dioxane (9.4 mL) was treated with 18 M aqueous hydrochloric acid solution (9.4 mL). The reaction mixture was heated to 120 °C for 18 h. At this time, the reaction mixture was cooled to 25 °C, diluted with water (100 mL), and extracted with 90/10 methylene chloride/methanol solution (3 × 100 mL). The organics were dried over sodium sulfate, filtered, and concentrated in vacuo. Flash chromatography (Merck silica gel 60, 230–400 mesh, ethyl acetate) afforded 2(R)-(3-chloro-4-methylsulfanyl-phenyl)-3-(2-oxo-cyclopentyl)-propionic acid **76** (1.54 g, 82%) as a yellow oil. EI-HRMS *m/e* calcd for C₁₅H₁₇ClO₃S (M)⁺, 312.0587; found, 312.0581. ¹H NMR (300 MHz, chloroform-*d*): δ 1.34–2.57 (m, 9 H), 2.47 (s, 3H), 3.63–3.99 (m, 1 H), 7.07–7.16 (m, 1 H), 7.19–7.26 (m, 1 H), 7.33 (dd, *J* = 6.23, 1.83 Hz, 1 H).

2(R)-(3-Chloro-4-methylsulfanyl-phenyl)-3-(2-oxo-cyclopentyl)-propionic Acid (**77**). A solution of 2(R)-(3-chloro-4-methylsulfanyl-phenyl)-3-(2-oxo-cyclopentyl)-propionic acid **76** (683.2 mg, 2.18

mmol), formic acid (2.47 mL, 65.5 mmol), and water (0.41 mL) cooled to 0 °C was treated with a 30% hydrogen peroxide solution (1.11 mL, 10.9 mmol). The reaction mixture stirred at 0 °C for 1 h. At this time, the reaction was treated with a saturated aqueous sodium sulfite solution. The resulting solution was poured into water (50 mL) and then extracted into methylene chloride (3 × 50 mL). The organics were dried over sodium sulfate, filtered, and concentrated in vacuo to afford 2(R)-(3-chloro-4-methylsulfanyl-phenyl)-3-(2-oxo-cyclopentyl)-propionic acid **77** (724 mg, 100%) as a white foam. EI-HRMS *m/e* calcd for C₁₅H₁₇ClO₄S (M + Na)⁺, 351.0428; found, 351.0433. ¹H NMR (300 MHz, chloroform-*d*): δ 1.37–2.58 (m, 9 H), 2.75–2.94 (m, 3 H), 3.77–4.09 (m, 1 H), 7.37–7.45 (m, 1 H), 7.49 (tdd, *J* = 6.50, 6.50, 3.30, 1.65 Hz, 1 H), 7.89 (d, *J* = 8.06 Hz, 1 H).

2(R)-(3-Chloro-4-methylsulfanyl-phenyl)-3-(2-oxo-cyclopentyl)-propionic Acid (**78**). A solution of potassium permanganate (101 mg, 0.64 mmol) in water (1.83 mL) was treated with a solution of 2(R)-(3-chloro-4-methylsulfanyl-phenyl)-3-(2-oxo-cyclopentyl)-propionic acid **77** (191.5 mg, 0.58 mmol) in methanol (5.8 mL). The reaction mixture was stirred at 25 °C for 1 h. At this time, the reaction mixture was diluted with methanol and filtered through a pad of Celite. The filtrate was concentrated and azeotroped with acetonitrile. Flash chromatography (Merck silica gel 60, 230–400 mesh, 90/10 methylene chloride/methanol 1% glacial acetic acid) afforded 2(R)-(3-chloro-4-methylsulfanyl-phenyl)-3-(2-oxo-cyclopentyl)-propionic acid **78** (87 mg, 43%) as an off white foam. EI-HRMS *m/e* calcd for C₁₅H₁₇ClO₅S (M – H₂O)⁺, 326.0379; found, 326.0378. ¹H NMR (300 MHz, chloroform-*d*): δ 1.33–2.60 (m, 9 H) 3.27 (s, 3 H) 3.79–4.21 (m, 1 H) 7.45 (ddd, *J* = 8.06, 4.76, 1.46 Hz, 1 H) 7.56 (dd, *J* = 4.76, 1.46 Hz, 1 H) 8.11 (d, *J* = 8.06 Hz, 1 H).

2(R)-(3-Chloro-4-methylsulfanyl-phenyl)-3-(2-oxo-cyclopentyl)-N-pyrazin-2-yl-propionamide (**29**). A solution of 2(R)-(3-chloro-4-methylsulfanyl-phenyl)-3-(2-oxo-cyclopentyl)-propionic acid **78** (125 mg, 0.36 mmol) in methylene chloride (3.62 mL) was cooled to 0 °C and was treated with a treated 2 M solution of oxalyl chloride in methylene chloride (0.20 mL, 0.39 mmol) and with a few drops of *N,N'*-dimethylformamide. The reaction mixture was then stirred at 0 °C for 10 min and at 25 °C for 20 min. The reaction mixture was then treated with a solution of 2-aminopyrazine (76 mg, 0.8 mmol) and pyridine (0.06 mL, 0.8 mmol) in anhydrous tetrahydrofuran (1.81 mL). The resulting reaction mixture was stirred at 25 °C for 1 h. At this time, the reaction mixture was concentrated in vacuo. Flash chromatography (Merck silica gel 60, 230–400 mesh, 75/25 ethyl acetate/hexanes) afforded 2(R)-(3-chloro-4-methylsulfanyl-phenyl)-3-(2-oxo-cyclopentyl)-N-pyrazin-2-yl-propionamide **29** (77.6 mg, 50.7%) as a white foam. EI-HRMS *m/e* calcd for C₁₉H₂₀ClN₃O₄S (M)⁺, 421.0863; found, 421.0868. ¹H NMR (300 MHz, chloroform-*d*): δ 1.42–2.49 (m, 9 H), 3.14–3.35 (m, 3 H), 4.21–4.41 (m, 1 H), 7.44–7.60 (m, 1 H), 7.67 (s, 1 H), 8.03–8.64 (m, 4 H), 9.50 (s, 1 H).

2(R)-(3-Chloro-4-methylsulfanyl-phenyl)-3-(2-hydroxy-cyclopentyl)-N-pyrazin-2-yl-propionamide (**27**). A solution of 2(R)-(3-chloro-4-methylsulfanyl-phenyl)-3-(2-oxo-cyclopentyl)-N-pyrazin-2-yl-propionamide **29** (13.5 mg, 0.03 mmol) in ethanol (0.32 mL) cooled to 0 °C was treated with sodium borohydride (1.2 mg, 0.3 mmol). The reaction mixture was stirred at 0 °C for 20 min. At this time, the reaction was diluted with water (25 mL). The mixture was extracted with ethyl acetate (3 × 30 mL). The combined organics were dried over sodium sulfate, filtered, and concentrated in vacuo. Flash chromatography (Merck silica gel 60, 230–400 mesh, ethyl acetate) afforded 2(R)-(3-chloro-4-methylsulfanyl-phenyl)-3-(2-hydroxy-cyclopentyl)-N-pyrazin-2-yl-propionamide **27** (10.1 mg, 75.5%) as a white foam. EI-HRMS *m/e* calcd for C₁₉H₂₂ClN₃O₄S (M + Na)⁺, 446.0912; found, 446.0916. ¹H NMR (300 MHz, chloroform-*d*): δ 1.10–2.58 (m, 9 H), 3.27 (s, 3 H), 3.74–4.08 (m, 2 H), 4.13 (m, *J* = 7.20, 7.20, 7.20 Hz, 1 H), 7.54 (d, *J* = 8.06 Hz, 1 H), 7.68 (d, *J* = 5.49 Hz, 1 H), 8.13 (d, *J* = 8.06 Hz, 1 H), 8.16–8.29 (m, 1 H), 8.36 (br. s., 1 H), 9.51 (br. s., 1 H).

2(R)-(3-Chloro-4-methylsulfanyl-phenyl)-N-[2(R)-hydroxy-1(R)-methyl-2(R)-phenyl-ethyl]-N-methyl-3-[3-(tetrahydro-pyran-2-yloxy)-cyclopentyl]-propionamide (**79**). A solution of 1,1,1,3,3,3-hexamethyldisilazane (3.75 mL, 17.24 mmol) in freshly distilled

tetrahydrofuran (50 mL) was treated slowly with a 2.3 M solution of *n*-butyllithium in hexanes (7.0 mL, 16.1 mmol) at -45°C . The resulting reaction solution was stirred at -40°C for 45 min and then treated slowly with a solution of 2-(3-chloro-4-methylsulfonyl-phenyl)-*N*-[2(*R*)-hydroxy-1(*R*)-methyl-2(*R*)-phenyl-ethyl]-*N*-methyl-acetamide **62** (2.5 g, 6.87 mmol) in tetrahydrofuran (10 mL) via a cannula. A yellow solution was obtained, and the reaction was allowed to warm to 0°C , where it was stirred for 30 min. This reaction solution was cooled to -50°C and treated with 1,3-dimethyl-3,4,5,6-tetrahydro-2(1*H*)-pyrimidinone (5 mL) followed by the dropwise addition of a solution of 2-(3-iodomethyl-cyclopentyloxy)-tetrahydropyran (prepared as in example 35, 3.2 g, 10.3 mmol) in tetrahydrofuran (10 mL). After the addition, the reaction solution was warmed to 0°C , where it was stirred for 2 h, and then warmed to 25°C , where it was stirred for an additional 2 h. The reaction solution was diluted with methylene chloride (100 mL) and washed with a saturated aqueous sodium chloride solution (100 mL). The organic layer was separated, dried over magnesium sulfate, filtered, and concentrated in vacuo. Flash chromatography (Merck Silica gel 60, 70–230 mesh, 40–60% ethyl acetate/hexanes) afforded 2(*R*)-(3-chloro-4-methylsulfonyl-phenyl)-*N*-(2(*R*)-hydroxy-1(*R*)-methyl-2(*R*)-phenyl-ethyl)-*N*-methyl-3-[3-(tetrahydro-pyran-2-yloxy)-cyclopentyl]-propionamide **79** (3.4 g, 90.7%) as a white solid. ^1H NMR (300 MHz, chloroform-*d*): δ 0.47–2.32 (m, 18 H), 2.44 (s, 3 H), 2.60–3.03 (m, 3 H), 3.27–4.76 (m, 7 H), 6.95–7.59 (m, 8 H).

2(*R*)-(3-Chloro-4-methylsulfonyl-phenyl)-3-(3-hydroxy-cyclopentyl)-propionic Acid (80). A solution of 2(*R*)-(3-chloro-4-methylsulfonyl-phenyl)-*N*-(2(*R*)-hydroxy-1(*R*)-methyl-2(*R*)-phenyl-ethyl)-*N*-methyl-3-[3-(tetrahydro-pyran-2-yloxy)-cyclopentyl]-propionamide **79** (0.96 g, 1.758 mmol) in dioxane (20 mL) was treated with a 9 N aqueous sulfuric acid solution (1.5 mL). The resulting reaction solution was heated under reflux for 15 h. In another flask, a solution of 2(*R*)-(3-chloro-4-methylsulfonyl-phenyl)-*N*-(2(*R*)-hydroxy-1(*R*)-methyl-2(*R*)-phenyl-ethyl)-*N*-methyl-3-[3-(tetrahydro-pyran-2-yloxy)-cyclopentyl]-propionamide (1 g, 1.83 mmol) in dioxane (20 mL) and a 9 N aqueous sulfuric acid solution (1.5 mL) was heated under reflux for 7 h. The two reactions were combined, diluted with methylene chloride (100 mL), and washed with a saturated aqueous sodium chloride solution (100 mL). The organic layer was separated, dried over magnesium sulfate, filtered, and concentrated in vacuo. Flash chromatography (Merck Silica gel 60, 70–230 mesh, 8–10% methanol/methylene chloride) afforded 2(*R*)-(3-chloro-4-methylsulfonyl-phenyl)-3-(3-hydroxy-cyclopentyl)-propionic acid **80** (496 mg, 43.9%) as an off-white foam. ^1H NMR (300 MHz, chloroform-*d*): δ 0.57–2.24 (m, 9 H), 2.45 (s, 3 H), 3.51 (t, $J = 7.51$ Hz, 1 H), 4.18–4.43 (m, 1 H), 6.94–7.55 (m, 3 H).

2(*R*)-(3-Chloro-4-methanesulfonyl-phenyl)-3-(3-formyloxy-cyclopentyl)-propionic Acid (81). A solution of 2(*R*)-(3-chloro-4-methylsulfonyl-phenyl)-3-(3-hydroxy-cyclopentyl)-propionic acid **80** (350 mg, 1.11 mmol) in formic acid (35 mL) was treated with a 30% aqueous hydrogen peroxide solution (1 mL, 7.89 mmol) at 25°C . The mixture was then allowed to stir at 25°C overnight. The solvent was evaporated in vacuo. The resulting residue was azeotroped with toluene to remove water and then coevaporated with *N,N*-dimethylformamide to remove formic acid to afford crude 2(*R*)-(3-chloro-4-methanesulfonyl-phenyl)-3-(3-formyloxy-cyclopentyl)-propionic acid **81** (430 mg, 103%) as an off-white solid. ^1H NMR (300 MHz, chloroform-*d*): δ 0.70–2.53 (m, 9 H), 3.28 (s, 3 H), 3.58–3.90 (m, 1 H), 5.08–5.46 (m, 1 H), 7.51 (d, $J = 8.06$ Hz, 1 H), 7.63 (s, 1 H), 8.13 (d, $J = 8.06$ Hz, 1 H), 8.22 (br. s., 1 H), 9.53 (br. s., 1 H).

3-[2(*R*)-(3-Chloro-4-methanesulfonyl-phenyl)-2-(pyrazin-2-ylcarbamoyl)-ethyl]-cyclopentyl Ester (82). A solution of 2(*R*)-(3-chloro-4-methanesulfonyl-phenyl)-3-(3-formyloxy-cyclopentyl)-propionic acid **81** (380 mg, 1.01 mmol) in toluene (10 mL) at 0°C was treated with *N,N*-dimethylformamide (0.008 mL) followed by a 2.0 M solution of oxalyl chloride in methylene chloride (0.75 mL). The reaction mixture was allowed to stir at 0°C for 30 min and at 25°C for 1.5 h. It appeared that a thick oil in the bottom of the reaction flask never solubilized. Additional methylene chloride (10 mL) was added at 25°C followed by *N,N*-dimethylformamide (0.002 mL) and oxalyl

chloride (0.3 mL). The reaction mixture was stirred at 25°C for an additional 45 min and then concentrated in vacuo. The residue was dissolved in dry tetrahydrofuran (5 mL) and cooled to 0°C . This cold solution was then treated with a solution of 2-aminopyrazine (142 mg, 1.5 mmol) and pyridine (0.121 mL, 1.5 mmol) in dry tetrahydrofuran (5 mL) via a cannula. The resulting reaction mixture was stirred at 0°C for 1 h and then diluted with methylene chloride (100 mL). The organic layer was successively washed with a 1 M aqueous citric acid solution (2×100 mL), a saturated sodium bicarbonate solution (1×100 mL), and a saturated sodium chloride solution (1×100 mL). The organics were dried over magnesium sulfate, filtered, and concentrated in vacuo to afford formic acid 3-[2(*R*)-(3-chloro-4-methanesulfonyl-phenyl)-2-(pyrazin-2-ylcarbamoyl)-ethyl]-cyclopentyl ester **82** (375 mg, 82%) as an off-white solid. ^1H NMR (300 MHz, chloroform-*d*): δ 0.73–2.49 (m, 9 H), 3.12–3.40 (m, 3 H), 3.53–3.91 (m, 1 H), 4.13–4.50 (m, 1 H), 5.41–6.22 (m, 1 H), 7.52 (d, $J = 8.06$ Hz, 1 H), 7.65 (s, 1 H), 8.12 (d, $J = 8.06$ Hz, 1 H), 8.17–8.45 (m, 2 H), 8.65–9.03 (m, 1 H), 9.54 (br. s., 1 H).

2(*R*)-(3-Chloro-4-methanesulfonyl-phenyl)-3-(3-hydroxy-cyclopentyl)-*N*-pyrazin-2-yl-propionamide (28). To a solution of formic acid 3-[2(*R*)-(3-chloro-4-methanesulfonyl-phenyl)-2-(pyrazin-2-ylcarbamoyl)-ethyl]-cyclopentyl ester **82** (375 mg, 0.83 mmol) in methanol (50 mL) at 0°C was bubbled ammonia gas for 15 min. The resulting reaction solution was stirred at 0°C for 15 min. The solvent was removed in vacuo. Flash chromatography (Merck Silica gel 60, 70–230 mesh, 1–5% methanol/methylene chloride) afforded 2(*R*)-(3-chloro-4-methanesulfonyl-phenyl)-3-(3-hydroxy-cyclopentyl)-*N*-pyrazin-2-yl-propionamide **28** (260 mg, 62.5%) as an off-white solid. ^1H NMR (300 MHz, methanol-*d*₄): δ 1.11–2.48 (m, 9 H), 3.19–3.44 (m, 3 H), 3.92–4.12 (m, 1 H), 4.14–4.40 (m, 1 H), 7.60–7.74 (m, 1 H), 7.75–7.86 (m, 1 H), 8.05–8.19 (m, 1 H), 8.27–8.35 (m, 1 H), 8.36–8.44 (m, 1 H), 9.41 (d, $J = 4.03$ Hz, 1 H).

2(*R*)-(3-Chloro-4-methanesulfonyl-phenyl)-3-(3-oxo-cyclopentyl)-*N*-pyrazin-2-yl-propionamide (30). A solution of 2(*R*)-(3-chloro-4-methanesulfonyl-phenyl)-3-(3-hydroxy-cyclopentyl)-*N*-pyrazin-2-yl-propionamide **28** (60 mg, 0.142 mmol) in methylene chloride (10 mL) was treated with Dess–Martin periodinane (1,1,1-Tris-(acetyloxy)-1,1-dihydro-1,2-benziodo-3-(1*H*)-one) (132.5 mg, 0.312 mmol). The reaction mixture was stirred at 25°C for 2 h. The reaction mixture was then diluted with methylene chloride (10 mL) and washed with a 1 M aqueous citric acid solution (10 mL). The pH of the aqueous layer was adjusted to 5. The aqueous layer was then extracted with methylene chloride (20 mL). The combined organic layers were dried over magnesium sulfate, filtered, and concentrated in vacuo. Flash chromatography (Merck Silica gel 60, 70–230 mesh, 50–100% ethyl acetate/hexanes) afforded 2(*R*)-(3-chloro-4-methanesulfonyl-phenyl)-3-(3-oxo-cyclopentyl)-*N*-pyrazin-2-yl-propionamide **30** (45 mg, 75%) as an off-white solid. ^1H NMR (300 MHz, methanol-*d*₄): δ 1.46–2.55 (m, 8 H), 3.19–3.43 (m, 4 H), 4.02–4.11 (m, 1 H), 7.69 (dd, $J = 8.42, 1.47$ Hz, 1 H), 7.81 (d, $J = 1.46$ Hz, 1 H), 8.06–8.15 (m, 1 H), 8.32 (d, $J = 2.56$ Hz, 1 H), 8.37 (dd, $J = 2.56, 1.46$ Hz, 1 H), 9.40 (t, $J = 1.28$ Hz, 1 H).

2(*R*),3(*R*)-Diphenyl-1,4-dioxo-spiro[4.4]non-6-ene (91). 2(*R*),3-(*R*)-Diphenyl-1,4-dioxo-spiro[4.4]non-6-ene **91** was obtained following the similar procedure described for **84** from 2-cyclopentene-1-one and (*R,R*)-hydrobenzoin **90**¹⁷ in toluene in 91.5% yield as a white solid. ^1H NMR (300 MHz, chloroform-*d*): δ 2.32–2.46 (m, 2 H), 2.54 (td, $J = 5.49, 2.93$ Hz, 2 H), 4.76 (s, 2 H), 5.93–6.07 (m, 1 H), 6.17–6.31 (m, 1 H), 7.20–7.29 (m, 5 H), 7.29–7.41 (m, 5 H).

1(*S*),5(*R*)-Bicyclo[3.1.0]hexan-2-spiro-2'-(4(*R*),5(*R*)-diphenyl dioxolane] (92). 1(*S*),5(*R*)-Bicyclo[3.1.0]hexan-2-spiro-2'-(4(*R*),5(*R*)-diphenyl dioxolane) **92** was obtained following the similar procedure described for **85** from 2(*R*),3(*R*)-diphenyl-1,4-dioxo-spiro[4.4]non-6-ene **91** in 68% yield after crystallization from pentane. HPLC (Zorbax XDB-C8 150 mm \times 5 mm, 5–100% acetonitrile/water + 0.1% trifluoroacetic acid, R_t 18.0 min) indicated 96.5 area % purity. ^1H NMR (300 MHz, chloroform-*d*): δ 0.56–0.83 (m, 2 H), 1.40–2.24 (m, 6 H), 4.65–4.86 (m, 2 H), 7.21 (dd, $J = 6.23, 2.93$ Hz, 2 H), 7.28–7.42 (m, 8 H).

7(S)-Iodomethyl-2(R),3(R)-diphenyl-1,4-dioxo-spiro[4.4]nonane (**93**). 7(S)-Iodomethyl-2(R),3(R)-diphenyl-1,4-dioxo-spiro[4.4]nonane **93** was obtained following the similar procedure described for **86** from 1(S),5(R)-bicyclo[3.1.0]hexan-2-spiro-2'-(4(R),5(R)-diphenyl dioxolane) **92** at 25 °C in 71.7% yield as a white solid.

2(R)-(3-Chloro-4-methylsulfanyl-phenyl)-3-(2(R),3(R)-diphenyl-1,4-dioxo-spiro[4.4]non-7(R)-yl)-N-(2(R)-hydroxy-1(R)-methyl-2-phenyl-ethyl)-N-methylpropionamide (**94**). 2(R)-(3-Chloro-4-methylsulfanyl-phenyl)-3-(2(R),3(R)-diphenyl-1,4-dioxo-spiro[4.4]non-7(R)-yl)-N-(2(R)-hydroxy-1(R)-methyl-2-phenyl-ethyl)-N-methylpropionamide **94** was obtained following the similar procedure described for **87** from 7(S)-iodomethyl-2(R),3(R)-diphenyl-1,4-dioxo-spiro[4.4]nonane **93** in 65% yield.

2(R)-(3-Chloro-4-methylsulfanyl-phenyl)-3-[(R)-3-oxo-cyclopentyl]-propionic Acid (**95**). 2(R)-(3-Chloro-4-methylsulfanyl-phenyl)-3-[(R)-3-oxo-cyclopentyl]-propionic acid **95** was obtained the similar procedure described for **88** from 2(R)-(3-chloro-4-methylsulfanyl-phenyl)-3-(2(R),3(R)-diphenyl-1,4-dioxo-spiro[4.4]non-7(R)-yl)-N-(2(R)-hydroxy-1(R)-methyl-2-phenyl-ethyl)-N-methylpropionamide **94** in 72% yield as a yellow foam. ¹H NMR (300 MHz, chloroform-*d*): δ 1.48–2.57 (m, 9 H), 2.48 (s, 3H), 3.53–3.63 (m, 1 H), 7.09–7.17 (m, 1 H), 7.22 (dd, *J* = 8.42, 2.20 Hz, 1 H), 7.35 (d, *J* = 1.83 Hz, 1 H).

2(R)-(3-Chloro-4-methanesulfonyl-phenyl)-3-[(R)-3-oxo-cyclopentyl]-propionic Acid (**96**). 2(R)-(3-Chloro-4-methanesulfonyl-phenyl)-3-[(R)-3-oxo-cyclopentyl]-propionic acid **96** was obtained following the similar procedure described for **89** from 2(R)-(3-chloro-4-methylsulfanyl-phenyl)-3-[(R)-3-oxo-cyclopentyl]-propionic acid **95** in 90% yield as a white solid. ¹H NMR (300 MHz, chloroform-*d*): δ 1.44–2.51 (m, 9 H), 3.28 (s, 3 H), 3.72 (t, *J* = 7.62 Hz, 1 H), 7.44 (dd, *J* = 8.31, 1.72 Hz, 1 H), 7.55 (d, *J* = 1.65 Hz, 1 H), 8.14 (d, *J* = 8.24 Hz, 1 H).

2(R)-(3-Chloro-4-methanesulfonyl-phenyl)-3-[(R)-3-oxo-cyclopentyl]-N-pyrazin-2-yl-propionamide (**4**). 2(R)-(3-Chloro-4-methanesulfonyl-phenyl)-3-[(R)-3-oxo-cyclopentyl]-N-pyrazin-2-yl-propionamide **4** was obtained following the similar procedure described for **31** from 2(R)-(3-chloro-4-methanesulfonyl-phenyl)-3-[(R)-3-oxo-cyclopentyl]-propionic acid **96** in 43% yield as a white foam. HPLC (Chiralpak AD-RH, 150 mm \times 5 mm, 5 ethanol/5 methanol/4 water, 60 min run, 220 nm, 0.5 cc/min, *R_t* of 2(R),3(S) = 25.4 min; 2(R),3(R) = 38.9 min) indicated 95.9 area% purity and >99% de. ¹H NMR (300 MHz, chloroform-*d*): δ 1.43–2.54 (m, 9 H), 3.29 (s, 3 H), 3.70 (t, *J* = 7.14 Hz, 1 H), 7.51 (dd, *J* = 8.17, 1.72 Hz, 1 H), 7.63 (d, *J* = 1.65 Hz, 1 H), 8.00 (s, 1 H), 8.17 (d, *J* = 8.10 Hz, 1 H), 8.23 (dd, *J* = 2.61, 1.51 Hz, 1 H), 8.39 (d, *J* = 2.47 Hz, 1 H), 9.52 (s, 1 H). Anal. (C₁₉H₂₀ClN₃O₄S) C, H, N, Cl, S.

GK in Vitro Enzyme Kinetics. The methods used to determine the effects of GK activators on GK enzymatic activity (*SC*_{1,5} and enzyme kinetic parameters *K_a*, α , and β) were previously described.² Various fixed concentrations of activators (ranging from ~0.010 to 30 μ M) were assayed in duplicate in the presence of a single, fixed concentration of glucose (5 mM) to determine the concentration of activator that causes a 1.5-fold increase in enzymatic activity relative to untreated GK. This term is called a stimulatory concentration (*SC*_{1,5}). To calculate an activator's effect of enzyme kinetic parameters, the activator was assayed in the presence of various fixed concentrations of glucose (0.8–50 mM). Apparent *V_{max}* and *S*_{0.5} (referred to *K_m* for an enzyme showing Michaelis–Menten kinetics) values were determined by fitting enzymatic rates to the Hill equation using GraphPad Prism version 5.01 for Windows, GraphPad Software, San Diego, CA).

Typical Microsomal Incubations. Pooled liver microsomes from mouse, rat, dog, monkey, and human (20 mg/mL) were purchased from Xenotech Inc. Incubation reaction mixtures contained a final concentration of 0.1 M potassium phosphate buffer (pH 7.4), 3 mM MgCl₂, 1 mM EDTA, 1 or 2 mg/mL microsomal protein, 20 μ M C-14 GK activator compounds, and 1 mM NADPH in a total volume of 1.0 mL. The incubations were conducted for 30 min with 5 min of preincubation after adding 10 μ L of 2 mM GK compound in methanol (total 1% methanol in incubation mixture), and reactions were terminated with 2 mL of ice cold methanol or 100 μ L of 50% aqueous TFA, after vortexes for 3 min, centrifuged at 3000 rpm at 4 °C for 10

min. The clear supernatant was used directly for HPLC radio-chromatography and mass spectral analysis. The samples were analyzed by Micromass Quattro Altima LCMS/MS using Water symmetry C18 column, 5.0 μ , 2.1 cm \times 15 cm.

In Vivo Studies in C57 Mice. Male C57Bl/6J mice (Jackson Laboratories), 15 weeks of age, were fasted for 19 h prior to the administration of oral dose of vehicle, 4 (5, 10, and 15 mg/kg). The OGTT (2 g/kg) was initiated 2 h following administration of vehicle or test compound. Blood obtained from a tail snip was collected in a heparinized capillary tube and used immediately to measure glucose levels using a YSI model 2700 Biochemistry Analyzer (YSI, Inc., Yellow Springs, OH). The formulation used for the in vivo study consisted of Gelucire44/14:ethanol:PEG400 (4:66:30 v/w/v). Food was withheld during the duration of the study, and mice had free access to water. All results are reported as the means \pm standard deviations (*n* = 6/time point). A Student's *t* test was used to test for statistical significance (*, *p* < 0.05). All animal procedures were approved by the Institutional Animal Care and Use Committee.

Toxicity Studies in Rats. Male Wistar rats were divided into three groups of vehicle, compound **1**, ent-**1**, with three animals per group. Each rat in compound **1** treatment group received 300 mg/kg dose, while in ent-**1** treatment group rats received 600 mg/kg dose, via oral administration. Blood was collected by cardiac puncture under isoflurane/O₂ conditions, before euthanization. After weighing, 2–3 sections of liver from the left lateral and medial lobes were fixed in 10% neutral-buffered formalin, processed in paraffin, sectioned, and stained with hematoxylin and eosin (H&E). The remaining liver was sliced, and systematic random samples were collected. Two to three sections of liver were snap-frozen in OCT for Oil Red O staining. Sections were examined microscopically.

■ ASSOCIATED CONTENT

■ Supporting Information

Synthesis of analogues 5–26, corresponding synthetic schemes (1–9), and efficacy figures (1 and 2) related to **1**, ent-**1**, and **2**. This material is available free of charge via the Internet at <http://pubs.acs.org>.

■ AUTHOR INFORMATION

Corresponding Author

*Tel: 973-235-3984. Fax: 973-235-2448. E-mail: ramakanth.sarabu@roche.com.

Notes

The authors declare no competing financial interest.

■ ACKNOWLEDGMENTS

We gratefully acknowledge all members of the Physical Chemistry Department for the characterization of the compounds and Formulations group for their support of in vivo experiments.

■ ABBREVIATIONS USED

ATP, adenosine triphosphate; GK, glucokinase; GKA, glucokinase activator; GSIR, glucose-stimulated insulin release; MODY-2, maturity onset diabetes of the young type 2; OGTT, oral glucose tolerance test; PHHI, persistent hyperinsulinemic hypoglycemia of infancy; PK, pharmacokinetics; *SC*_{1,5}, concentration of a compound that increases GK activity by 1.5 times over the untreated GK; T2D, type 2 diabetes

■ REFERENCES

(1) Matschinsky, F. M. Assessing the potential of glucokinase activators in diabetes therapy. *Nat. Rev. Drug Discovery* **2009**, *8*, 399–416.

- (2) Matschinsky, F. M.; Ellerman, J. E. Metabolism of glucose in islets of Langerhans. *J. Biol. Chem.* **1968**, *243*, 2730–2736.
- (3) (a) Sharma, C.; Manjeshwar, R.; Weinhouse, S. Hormonal and dietary regulation of hepatic glucokinase. *Adv. Enzyme Regul.* **1964**, *2*, 189–200. (b) Van Schaftingen, E. A protein from rat liver confers to glucokinase the property of being antagonistically regulated by fructose 6-phosphate and fructose 1-phosphate. *Eur. J. Biochem.* **1989**, *179*, 179–184.
- (4) Matschinsky, F. M.; Magnuson, M. A.; Zelent, D.; Jetton, T. L.; Doliba, N.; Han, Y.; Taub, R.; Grimsby, J. The network of glucokinase-expressing cells in glucose homeostasis and the potential of glucokinase activators for diabetes therapy. *Diabetes* **2006**, *55*, 1–12.
- (5) Edghill, E. L.; Hattersley, A. T. Genetic disorders of the pancreatic beta cell and diabetes (Permanent neonatal diabetes and maturity onset diabetes of the young). In *Pancreatic Beta Cell in Health and Disease*; Seino, S., Bell, G. I., Eds.; Springer: Tokyo, 2008; pp 399–430.
- (6) Glaser, B.; Kesavan, P.; Heyman, M.; Davis, E.; Cuesta, A.; Buchs, A.; Stanley, C. A.; Thornton, P. S.; Permutt, M. A.; Matschinsky, F. M.; Herold, K. C. Familial hyperinsulinism caused by an activating glucokinase mutation. *N. Engl. J. Med.* **1998**, *338*, 226–230.
- (7) (a) Grimsby, J.; Sarabu, R.; Corbett, W. L.; Haynes, N. E.; Bizzarro, F. T.; Coffey, J. W.; Guertin, K. R.; Hilliard, D. H.; Kester, R. F.; Mahaney, P. E.; Marcus, L.; Qi, L.; Spence, C. L.; Teng, J.; Magnuson, M. A.; Chu, C. A.; Dvornozniak, M. T.; Matschinsky, F. M.; Grippo, J. F. Allosteric activators of glucokinase: Potential role in diabetes therapy. *Science* **2003**, *301*, 370–373. (b) Grimsby, J.; Zhi, J.; Mulligan, M. E.; Arbet-Engels, C.; Taub, R.; Balena, R. Presented at the Keystone Symposia: Diabetes Mellitus, Insulin Action and Resistance, January 2008, Breckenridge, CO, United States, poster 151. (c) Haynes, N. E.; Corbett, W. L.; Bizzarro, F. T.; Guertin, K. G.; Hilliard, D. W.; Holland, G. W.; Kester, R. F. K.; Mahaney, P. E.; Qi, L.; Spence, C. L.; Teng, J.; Dvornozniak, M. T.; Railkar, A.; Matschinsky, F. M.; Grippo, J. F.; Grimsby, J. G.; Sarabu, R. Discovery, structure-activity relationships, pharmacokinetics, and efficacy of glucokinase activator (2R)-3-cyclopentyl-2-(4-methanesulfonylphenyl)-N-thiazol-2-yl-propionamide. *J. Med. Chem.* **2010**, *53*, 3618–3625.
- (8) (a) Kester, R. F.; Corbett, W. L.; Sarabu, R.; Mahaney, P. E.; Haynes, N. E.; Guertin, K. R.; Bizzarro, F. T.; Hilliard, D. W.; Qi, L.; Teng, J.; Grippo, J. F.; Grimsby, J.; Marcus, L.; Dvornozniak, M.; Racha, J.; Wang, K. Discovery of piragliatin, a small molecule activator of GK (MEDI-005). 238th ACS National Meeting, Washington DC, August 16–20, 2009. (b) Sarabu, R.; Tilley, J. W.; Grimsby, J. The discovery of piragliatin, a glucokinase activator. *RSC Drug Discovery Ser.* **2011**, *4*, 51–70.
- (9) Myers, A. G.; Yang, H. B.; Chen, H.; Gleason, J. L. Use of pseudoephedrine as a practical chiral auxiliary for symmetric synthesis. *J. Am. Chem. Soc.* **1994**, *116*, 9361–9362.
- (10) Miller, R. D.; McKean, D. R. Ring opening of cyclopropyl ketones by trimethylsilyl iodide. *J. Org. Chem.* **1981**, *46*, 2412–2414.
- (11) Mash, E. A.; Torok, D. S. Homochiral ketals in organic Synthesis. Diastereoselective cyclopropanation of α,β -unsaturated ketals derived from (S,S)-(-)-hydrobenzoin. *J. Org. Chem.* **1989**, *54*, 250–253.
- (12) Dieter, R. K.; Pounds, S. Ring-opening reactions of electrophilic cyclopropanes. *J. Org. Chem.* **1982**, *47*, 3174–3177.
- (13) O'Doherty, R. M.; Lehman, D. L.; Telemaque-Potts, S.; Newgard, C. B. Metabolic impact of glucokinase overexpression in liver: Lowering of blood glucose in fed rats is accompanied by hyperlipidemia. *Diabetes* **1999**, *48*, 2022–2027.
- (14) See, for example (a) Mizutani, T.; Yoshida, K.; Kawazoe, S. Formation of toxic metabolites from thiazibendazole and other thiazoles in mice. *Drug Metab. Dispos.* **1994**, *22*, 750–755. (b) Stevens, G. J.; Hitchcock, K.; Wang, Y. K.; Coppola, G. M.; Versace, R. W.; Chin, J. A.; Shapiro, M.; Suwanrumpha, S.; Mangold, L. K. *In vitro* metabolism of N-(5-chloro-2-methylphenyl)-N-(2-methylpropyl)thiourea: Species comparison and identification of a novel thiocarbamide-glutathione adduct. *Chem. Res. Toxicol.* **1997**, *10*, 733–741.
- (15) Bonadonna, R. C.; Heise, T.; Arbet-Engels, C.; Kapitza, C.; Avogaro, A.; Grimsby, J.; Zhi, J.; Grippo, J. F.; Balena, R. Piragliatin (RO4389620), a novel glucokinase activator, lowers plasma glucose both in the postabsorptive state and after a glucose challenge in patients with type 2 diabetes mellitus: A mechanistic study. *J. Clin. Endocrinol. Metab.* **2010**, *95*, 5028–5036.
- (16) <http://www.scripintelligence.com/home/Roche-licenses-GKA-diabetes-candidates-to-Chinas-Hua-Medicine-325220>.
- (17) Wang, Z. M.; Sharpless, K. B. A Solid-to-solid asymmetric dihydroxylation procedure for kilogram-scale preparation of enantiopure hydrobenzoin. *J. Org. Chem.* **1994**, *59*, 8302–8303.